Supporting material

Integrating experimental and theoretical approaches to unveil structure–bioactivity relationships in silver(I) *N*-substituted glycine complexes

Gabriela Kuzderová, Róbert Gyepes, Alan Liška, Jana Havlíčková, Mária Vilková, Simona Žiláková, Martin Kello, Tomáš Pagáč, Petra Olejníková, Eva Petrovová, Ľudmila Balažová, Henrieta Matajová, Mária Kožurková, Danica Sabolová, Michaela Rendošová, Zuzana Vargová*

Abstract

N-methyl and *N*-glycyl glycine derivatives - namely (trimethylammonium)acetate (*N,N,N*-trimethylglycine, betaine, Bet), *N,N*-dimethylglycine (Dmg), *N*-methylglycine (sarcosine, Sar), and glycylglycylglycine (GlyGlyGly) - as naturally occurring glycine metabolites, were employed as stabilizing ligands for silver(I) ions, leading to the formation of water-soluble polymeric coordination compounds: $\{[Ag(HSar)(NO_3)]\}_n$ (AgSar), $\{[Ag(HDmg)(NO_3)]\}_n$ (AgDmg), $\{[Ag_3(HBet)_2(NO_3)_3]\}_n$ (AgBet), and [Ag(HGlyGlyGly)(NO_3)] (AgGlyGlyGly). The composition and structures of the resulting complexes were unambiguously confirmed using attenuated total reflection Fourier-transform infrared spectroscopy (ATR-FTIR), elemental analysis, thermogravimetric analysis (TGA), and single-crystal X-ray diffraction (SC-XRD). Speciation and stability studies in relevant test and growth media were conducted through potentiometric titrations, electrochemical measurements, ^{1}H NMR and UV–Vis spectroscopy and supported by theoretical calculations. All complexes demonstrated significantly enhanced antistaphylococcal activity compared to silver(I) nitrate ($AgNO_3$), with AgBet and AgGlyGlyGly exhibiting approximately 10-fold, and AgSar and AgDmg approximately 5-fold, increased efficacy. Moreover, AgBet and AgGlyGlyGly were nearly twice as active as silver(I) sulfadiazine (AgSD), a clinically used but poorly water-soluble antimicrobial agent. Remarkably, AgBet and AgGlyGlyGly also showed potent antifungal activity, being 10- to 100-fold more effective than both $AgNO_3$ and AgSD against *Rhizopus oryzae*, the causative agent of mucormycosis. In cytotoxicity assays, AgSar exhibited the greatest selectivity and sensitivity, being over three times higher than cisPt, against the human breast adenocarcinoma cell line MDA-MB-231. Structure–activity relationships and bioavailability were further explored via human serum albumin (HSA) binding studies, as well as experimental and computational evaluations of lipophilicity and additional Lipinski's parameters. Furthermore, the silver(I) complexes action mechanism was assessed via β-galactosidase inhibition and PCR amplification inhibition in *E. coli*, intracellular reactive oxygen species (ROS) production, and their effects on cell cycle progression and binding to ctDNA.

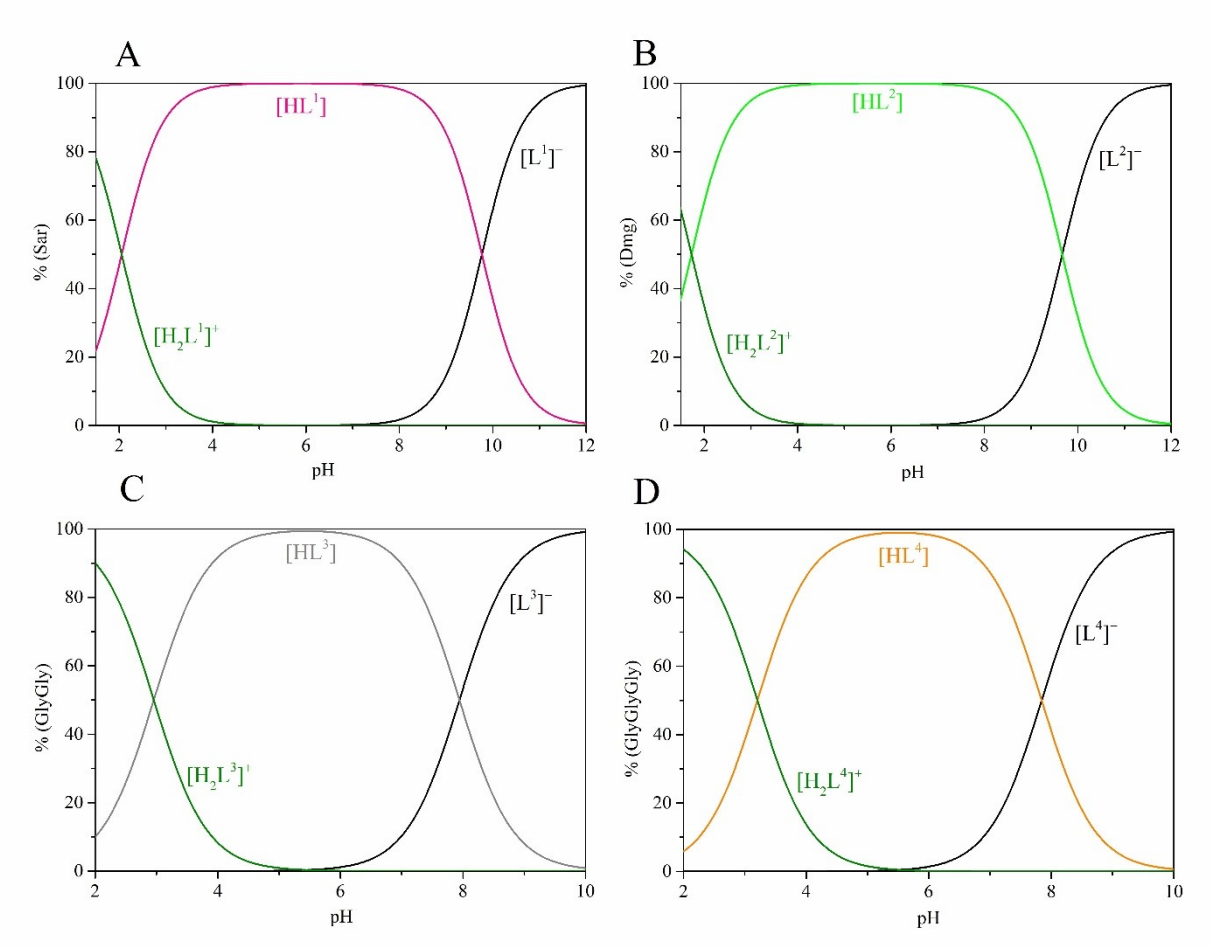

Figure S1 Distribution of Sar (A), Dmg (B), GlyGly (C) and GlyGlyGly (D) species in aqueous solution ($c(L^{1\text{-}4})$ = 4 mM), I = 0.1 M, 25 °C, (L^1 = Sar, L^2 = Dmg, L^3 = GlyGly, L^4 = GlyGlyGly)

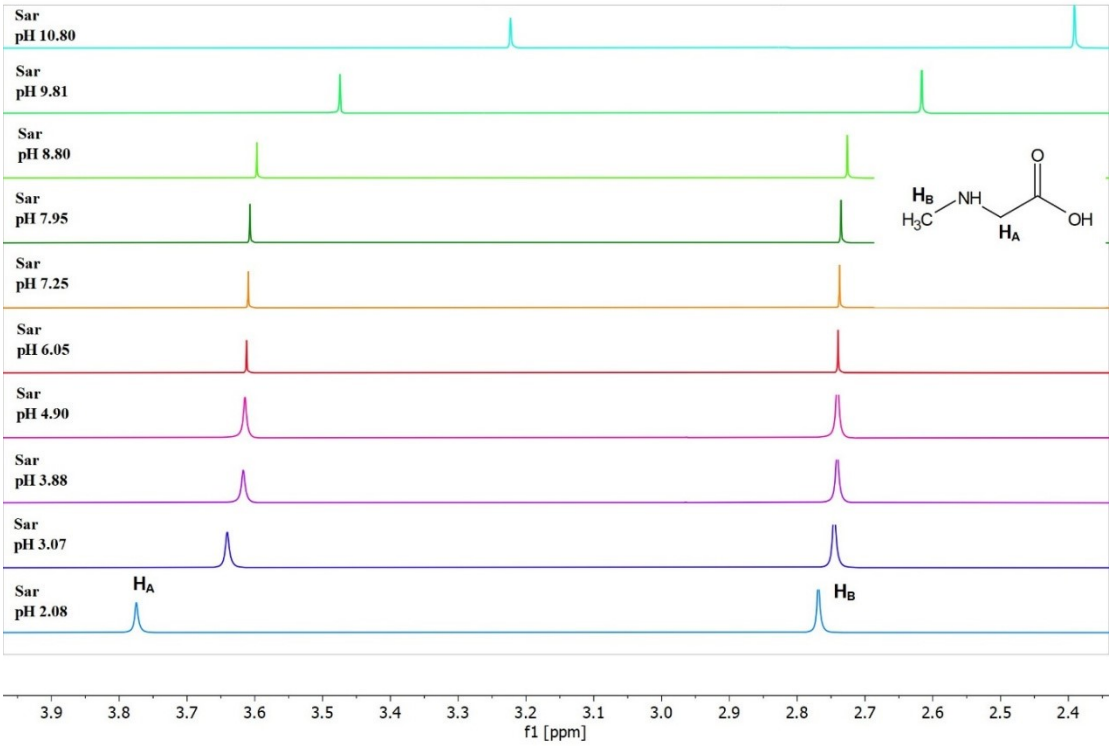

Figure S2 ^{1}H NMR titration spectra of an aqueous solution of the Sar ligand as a function of pH (*c*(Sar) = 50 mM)

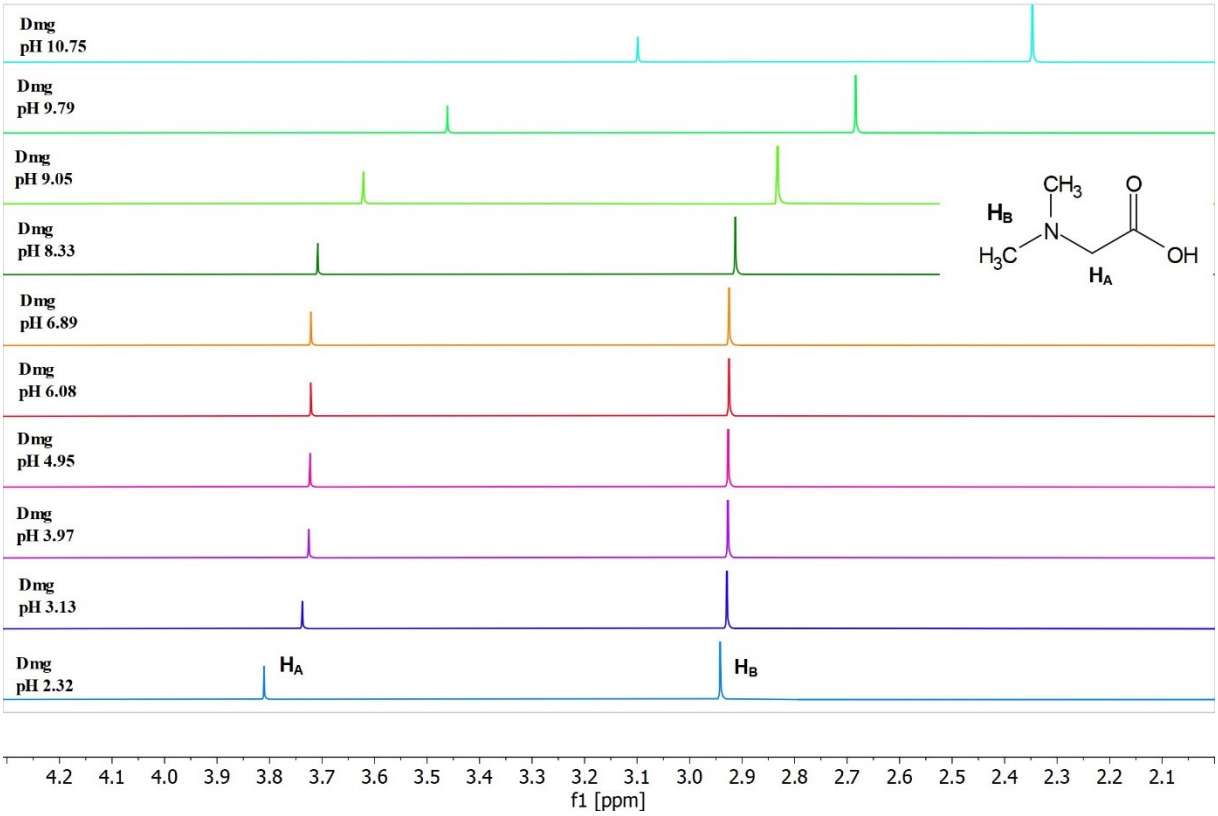

Figure S3 ^{1}H NMR titration spectra of an aqueous solution of the Dmg ligand as a function of pH (*c*(Dmg) = 50 mM)

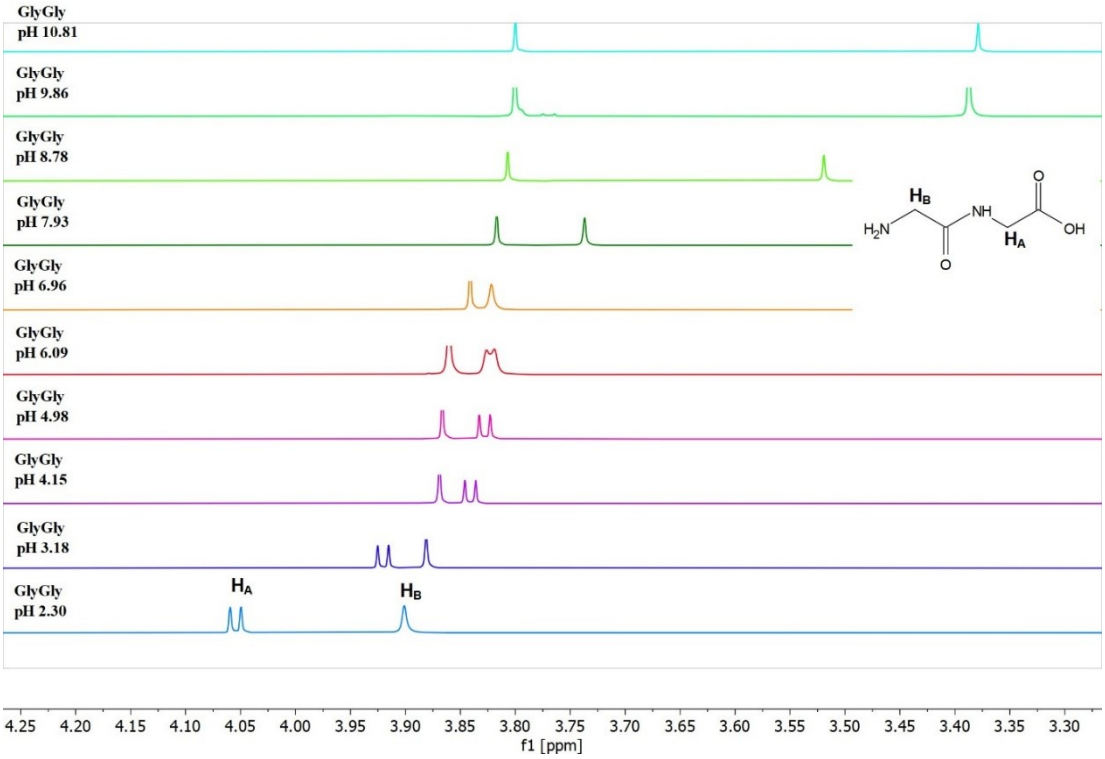

Figure S4 [1]H NMR titration spectra of an aqueous solution of the GlyGly ligand as a function of pH (*c*(GlyGly) = 50 mM)

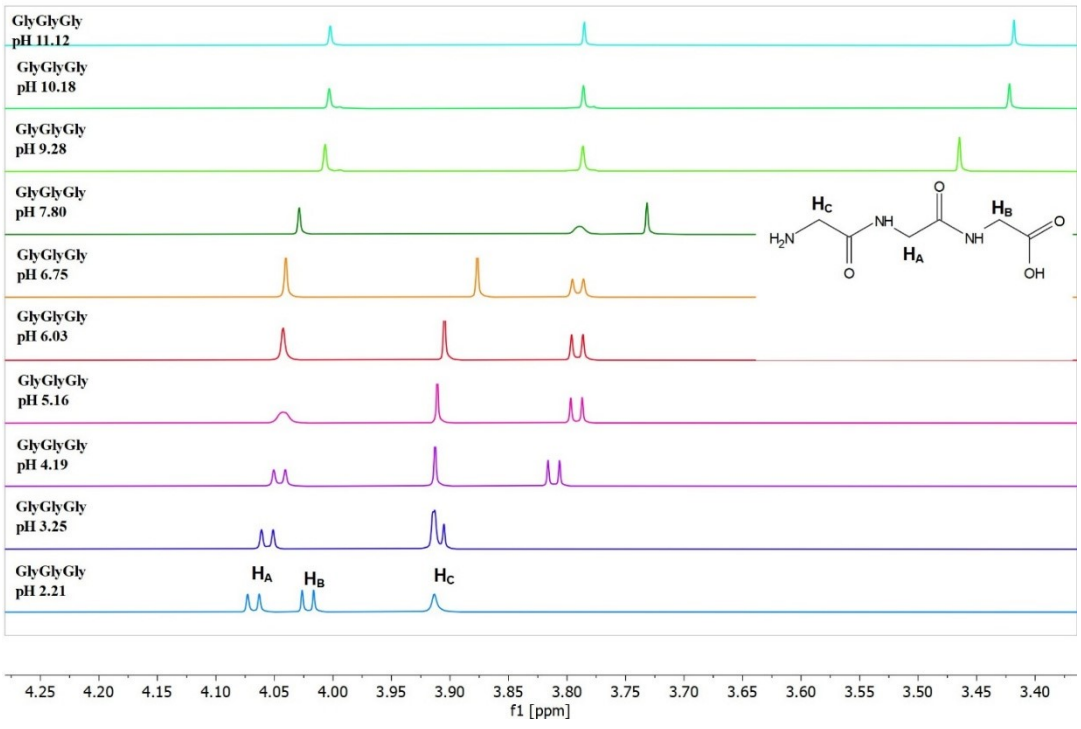

Figure S5 [1]H NMR spectra of an aqueous solution of the GlyGlyGly ligand as a function of pH (*c*(GlyGlyGly) = 50 mM)

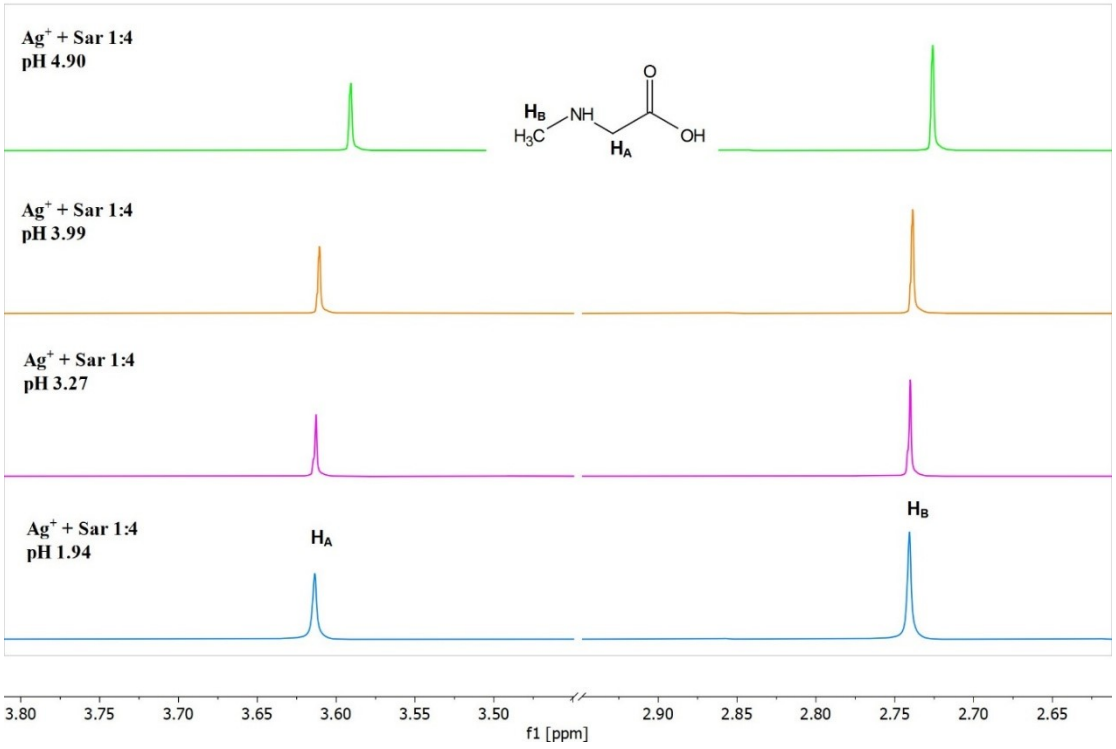

Figure S6 ^{1}H NMR titration spectra of an aqueous solution of the Ag(I)-Sar system (molar ratio 1:4) as a function of pH (c(Ag(I)) = 25 mM, Sar = 25 mM)

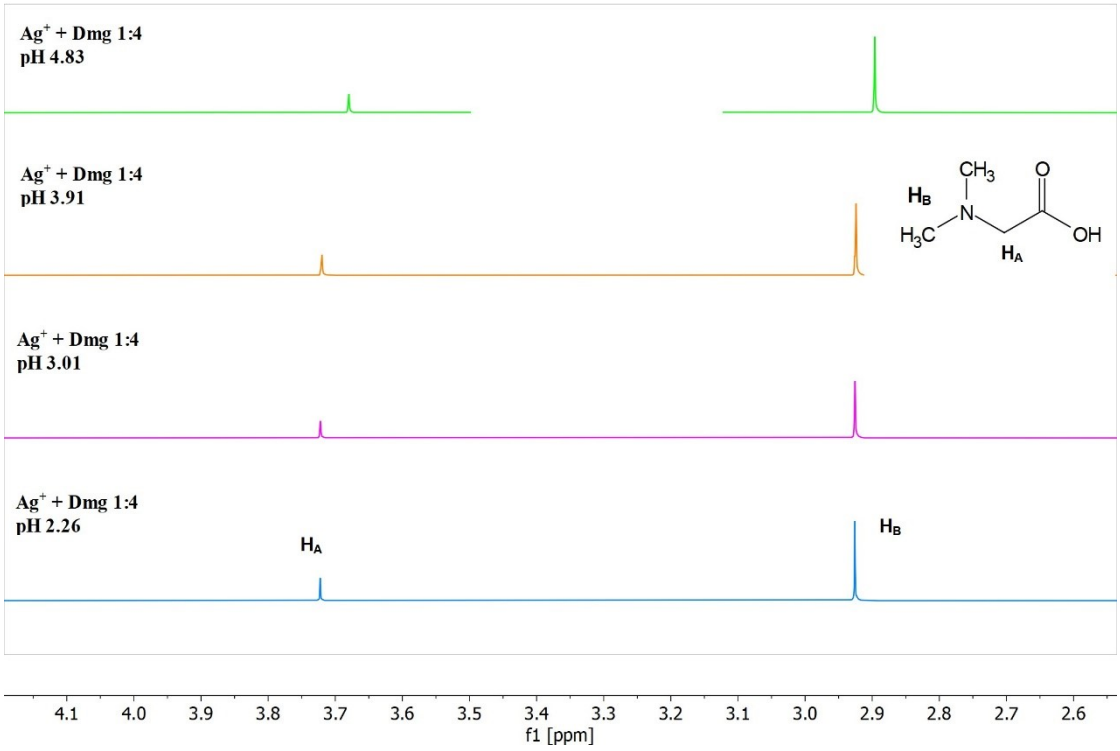

Figure S7 ^{1}H NMR spectra of an aqueous solution of the Ag(I)-Dmg system (molar ratio 1:4) as a function of pH (c(Ag(I)) = 25 mM, Dmg = 25 mM)

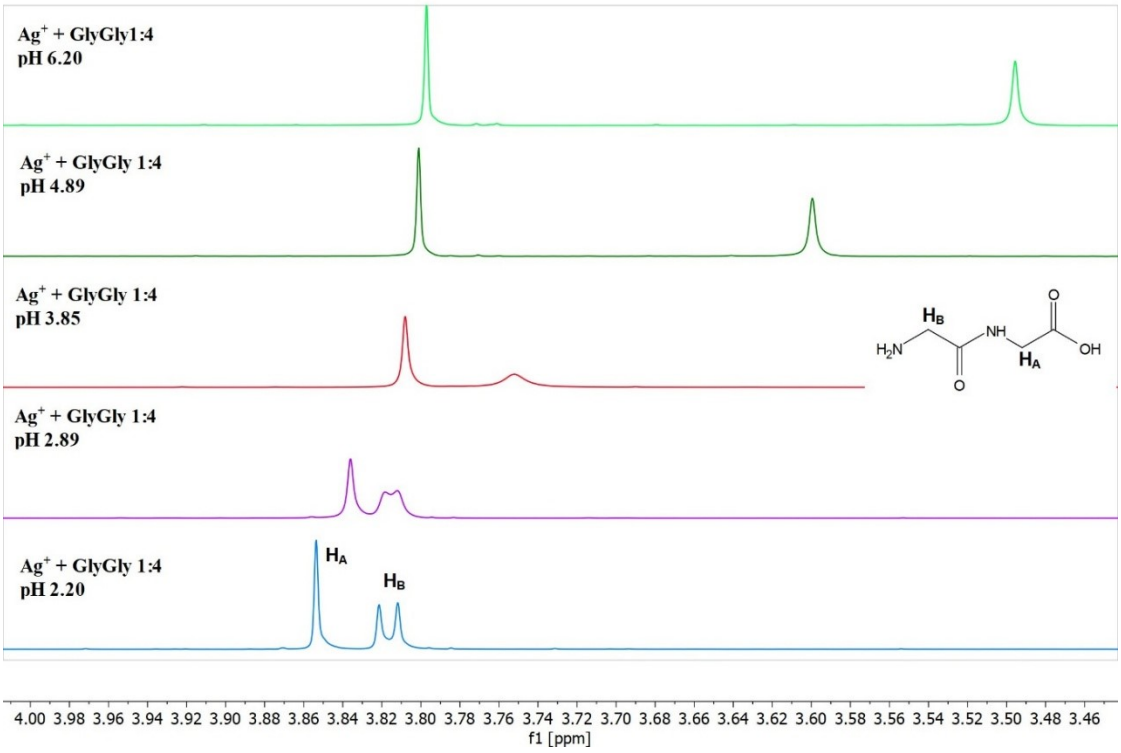

Figure S8 [1]H NMR spectra of an aqueous solution of the Ag(I)-GlyGly system (molar ratio 1:4) as a function of pH (c(Ag(I)) = 25 mM, GlyGly = 25 mM)

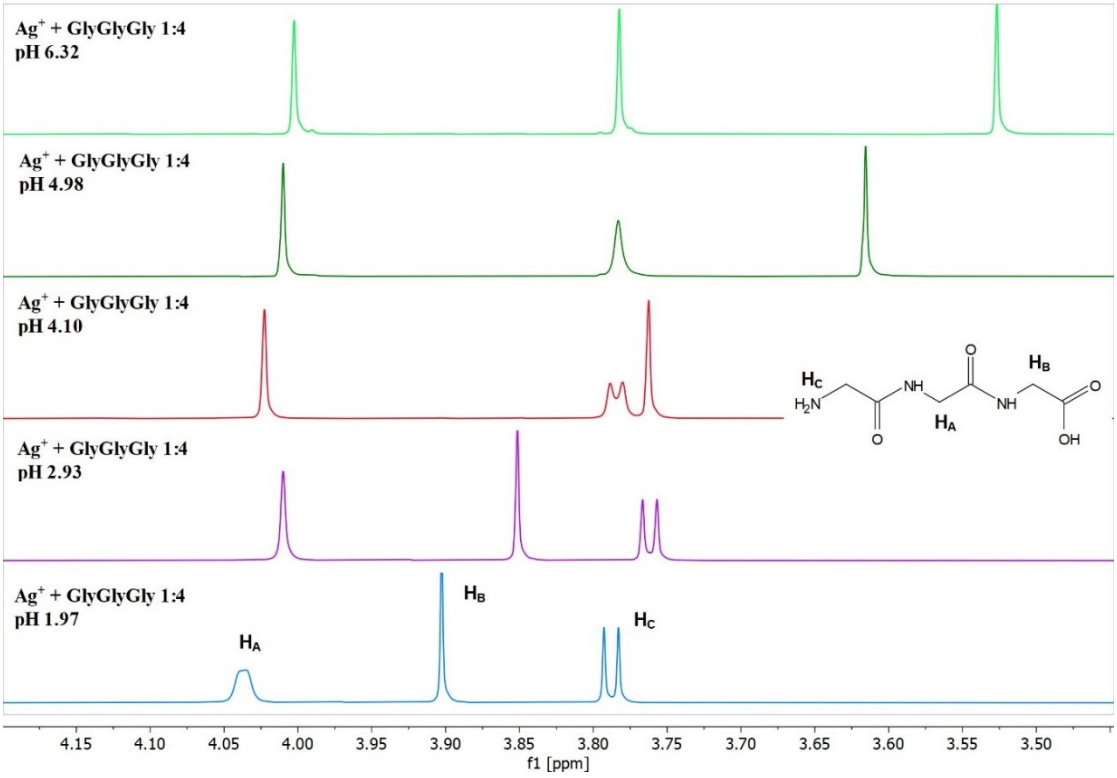

Figure S9 [1]H NMR spectra of an aqueous solution of the Ag(I)-GlyGlyGly system (molar ratio 1:4) as a function of pH (c(Ag(I)) = 25 mM, GlyGlyGly = 25 mM)

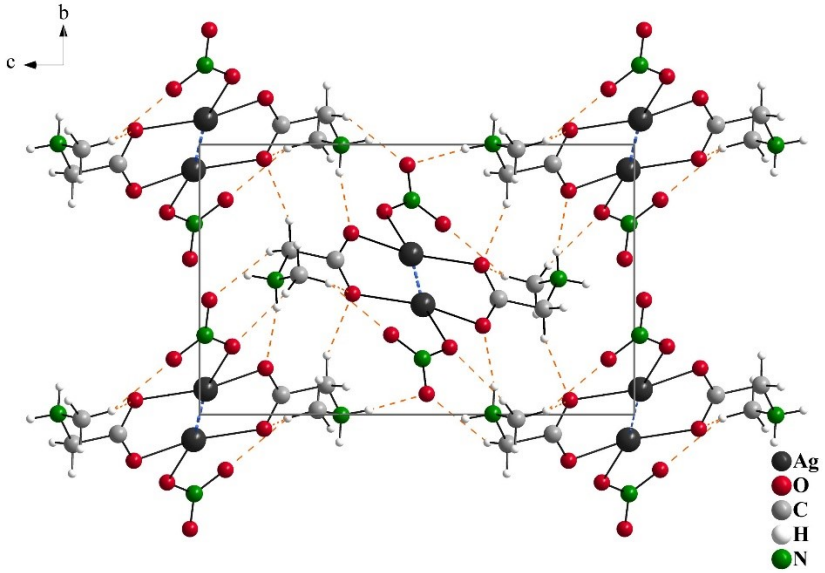

Figure S10 Solid-state packing viewed along [100] for AgSar with argentophilic interactions (blue dashed lines) and the hydrogen bond system (orange dashed lines).

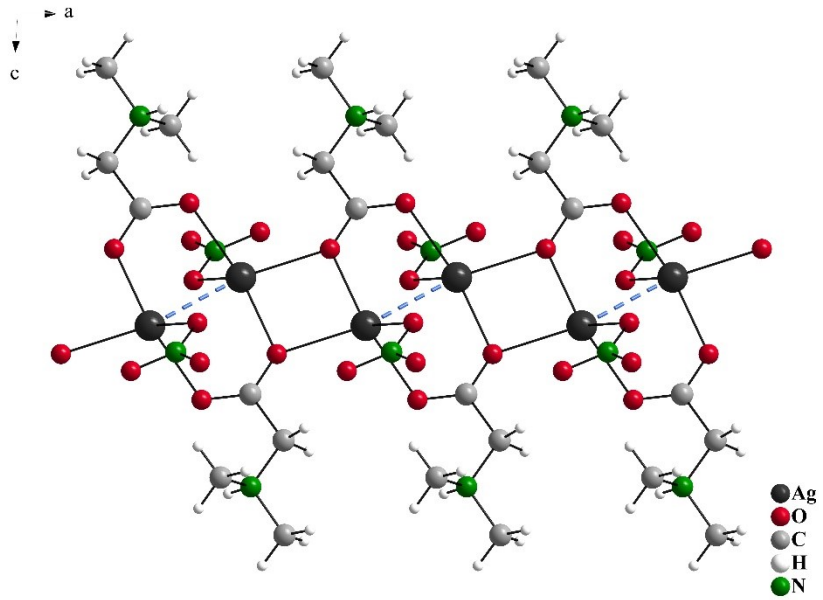

Figure S11 View of the propagation of 1D chain along a axis for AgDmg with argentophilic interactions (blue dashed lines)

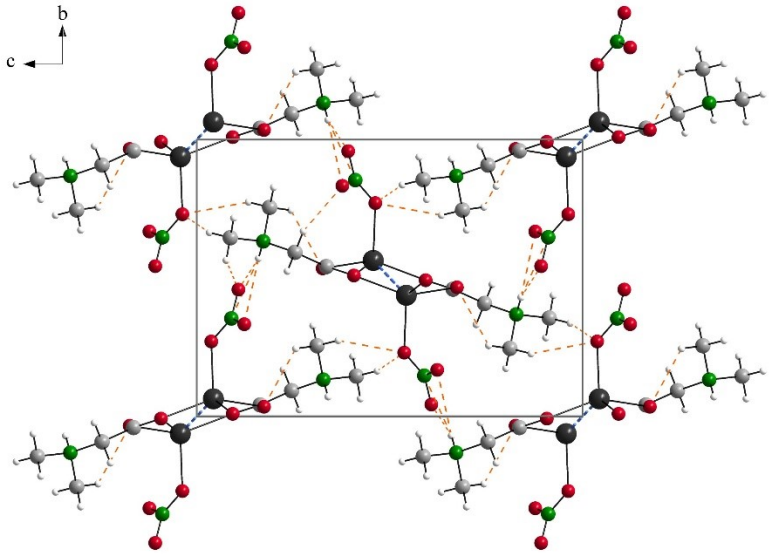

Figure S12 Solid-state packing viewed along [100] for AgDmg with argentophilic interactions (blue dashed lines) and the hydrogen bond system (orange dashed lines).

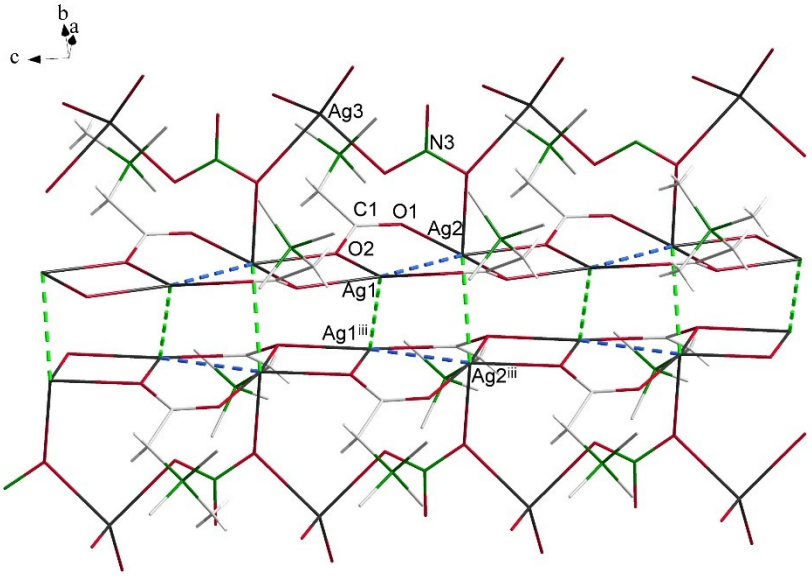

Figure S13 View of the propagation of 1D chain along c axis (hydrogen atoms are omitted for clarity) in double layered structure of AgBet with significant argentophilic interactions (blue and green dashed bonds)

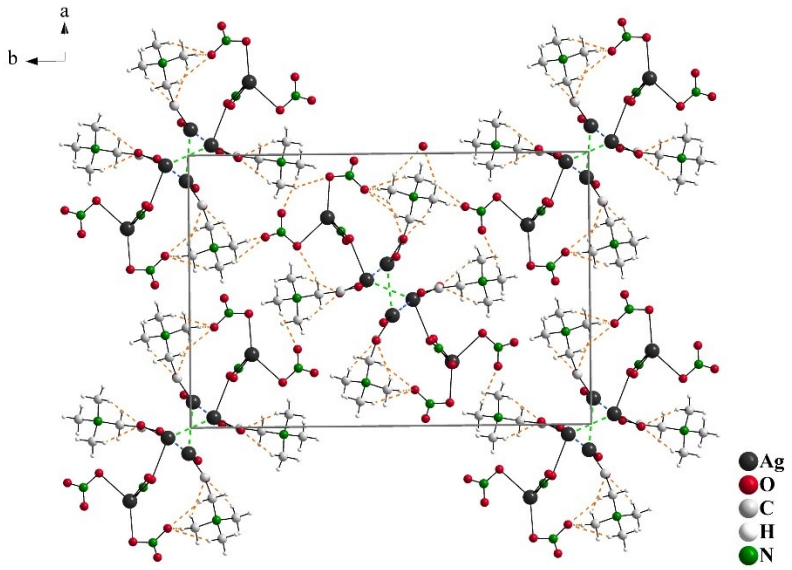

Figure S14 Solid state packing viewed along [001] (B) for AgBet with argentophilic interactions (blue and green dashed bonds) and the hydrogen bond system (orange dashed bonds)

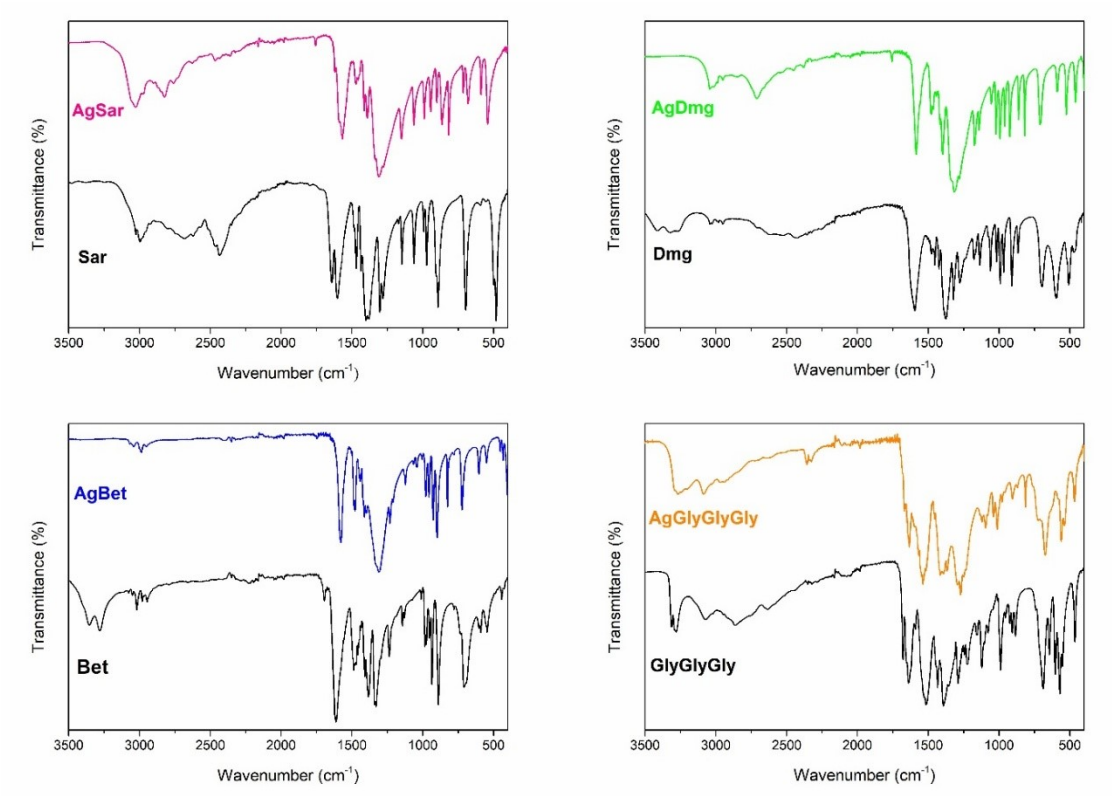

Figure S15 IR spectra of ligands Sar, Dmg, Bet, GlyGlyGly (black lines) and their silver(I) complexes AgSar (pink line), AgDmg (green line), AgBet (blue line) and AgGlyGlyGly (orange line)

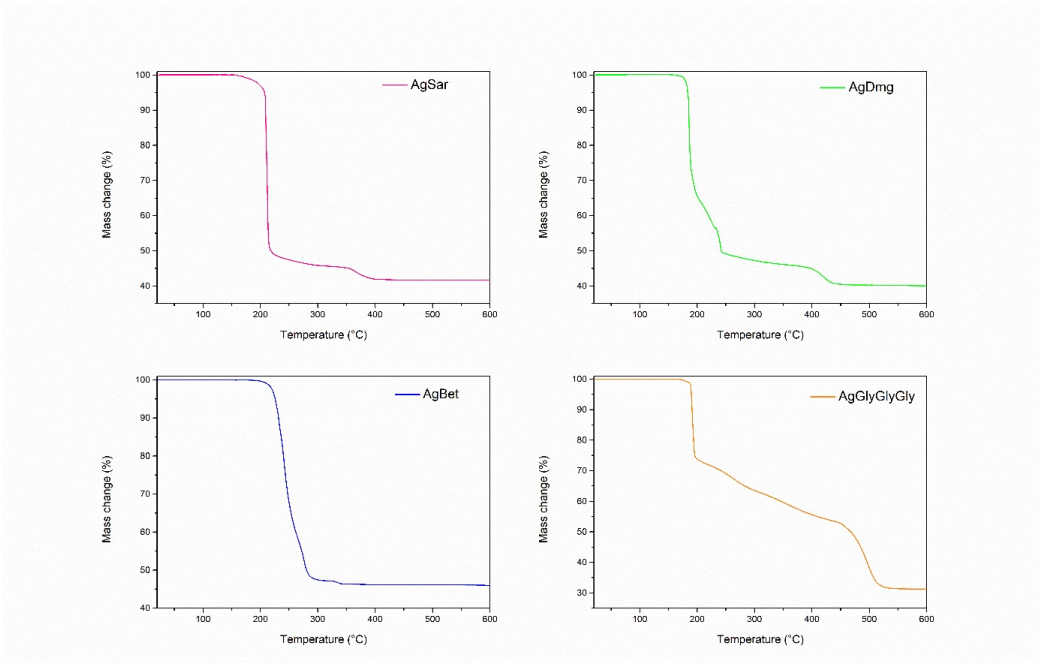

Figure S16 Thermogravimetric curves for studied silver(I) complexes measured in the air atmosphere in the temperature range of 25–600 °C

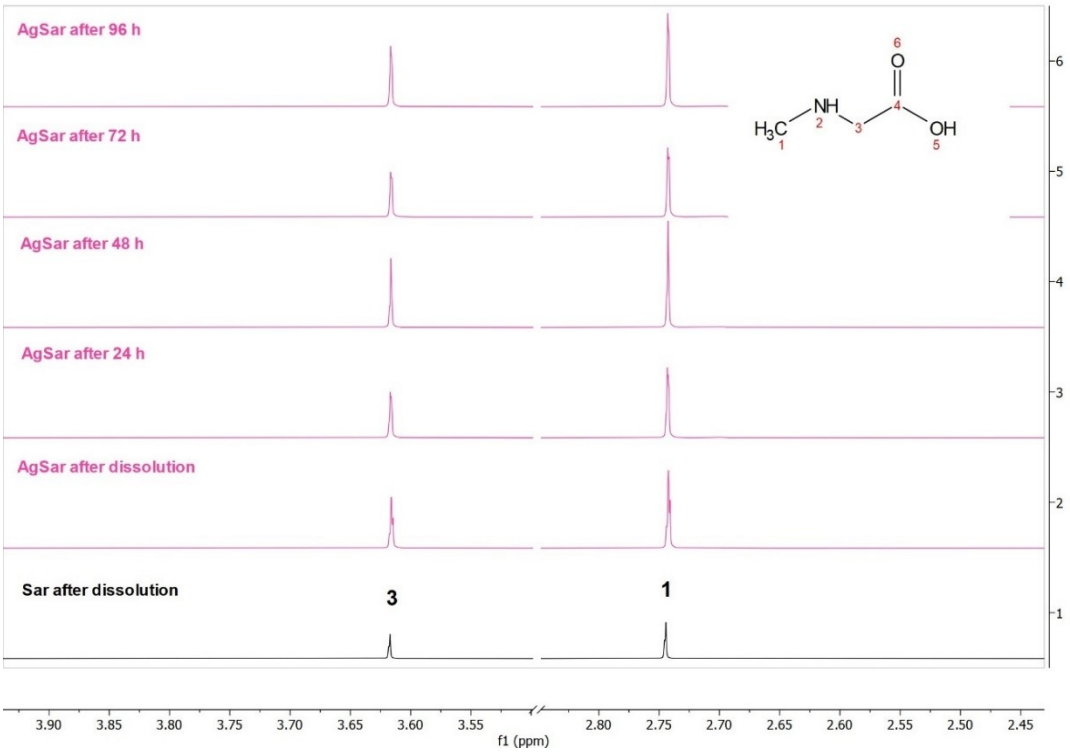

Figure S17 ^{1}H NMR spectrum of the Sar ligand after dissolution, and ^{1}H NMR spectra of the AgSar complex measured over a period of four days after dissolution in 1%DMSO

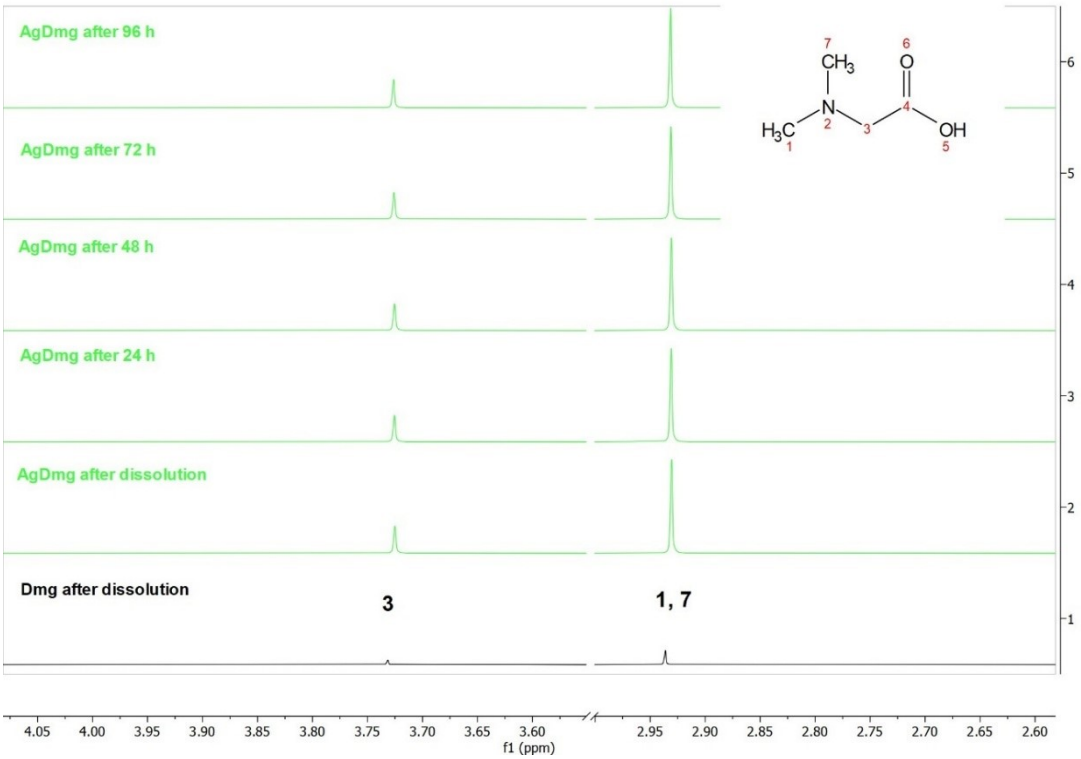

Figure S18 Dmg ligand ^{1}H NMR spectrum after its dissolution and AgDmg complex ^{1}H NMR spectra after its dissolution and measured over a period of four days in 1%DMSO

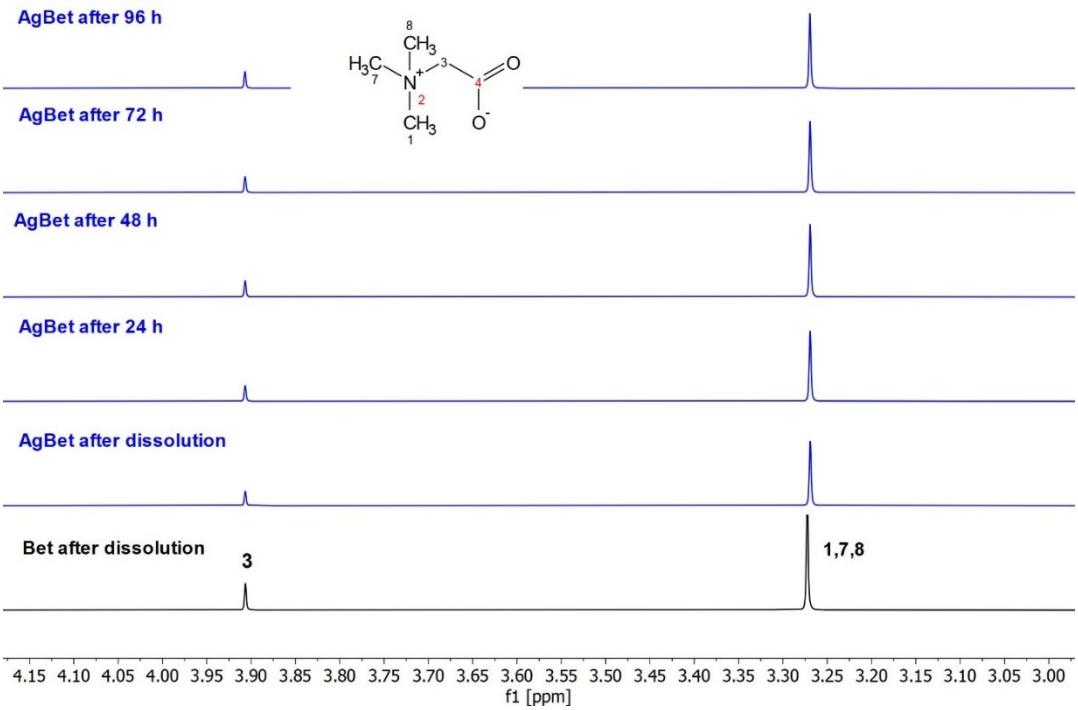

Figure S19 ^{1}H NMR spectrum of the Bet ligand (pH = 4–5) after dissolution, ^{1}H NMR spectra of the AgBet complex (pH = 4–5) measured over a period of four days after dissolution in 1%DMSO

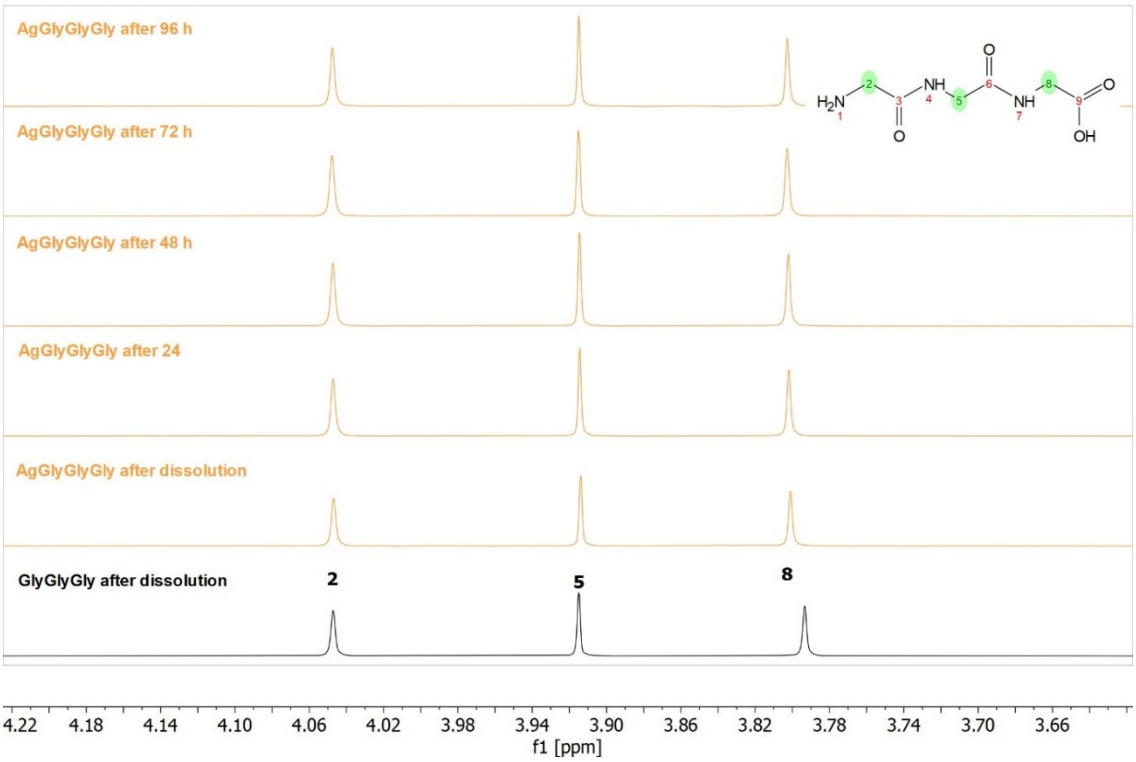

Figure S20 ^{1}H NMR spectrum of the GlyGlyGly ligand after dissolution, and ^{1}H NMR spectra of the AgGlyGlyGly complex (pH = 5) measured over a period of four days after dissolution in 1%DMSO

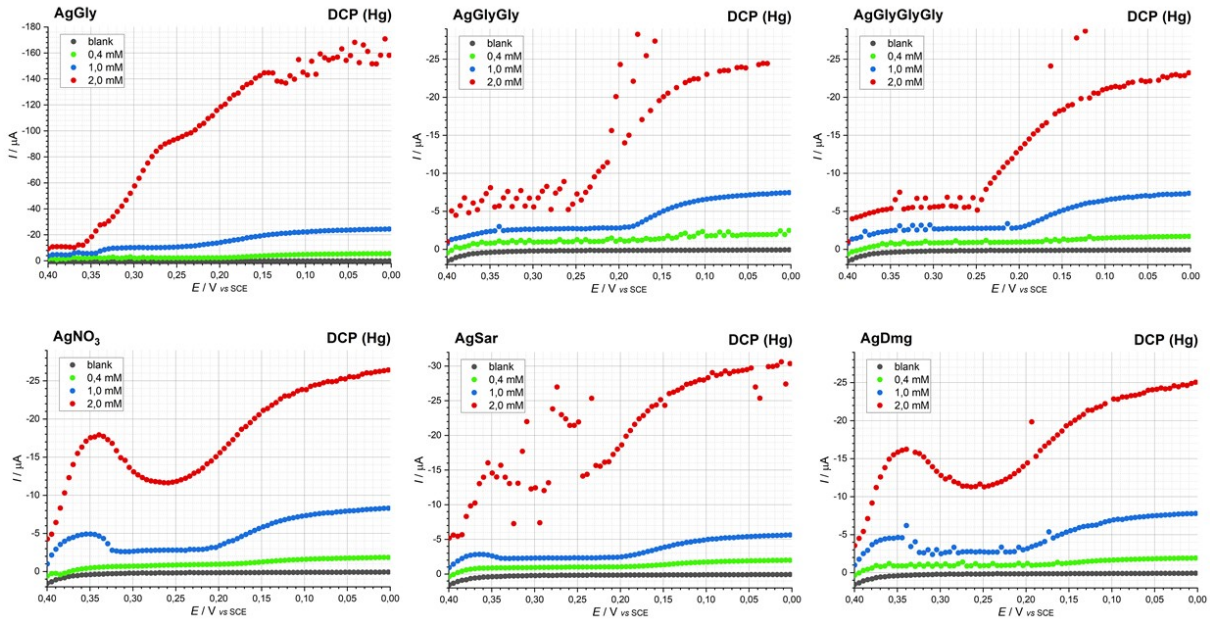

Figure S21 DC-polarography of the studied Ag(I) compounds measured in the defined concentration values of the solutions 0.4, 1.0 and 2.0 mM

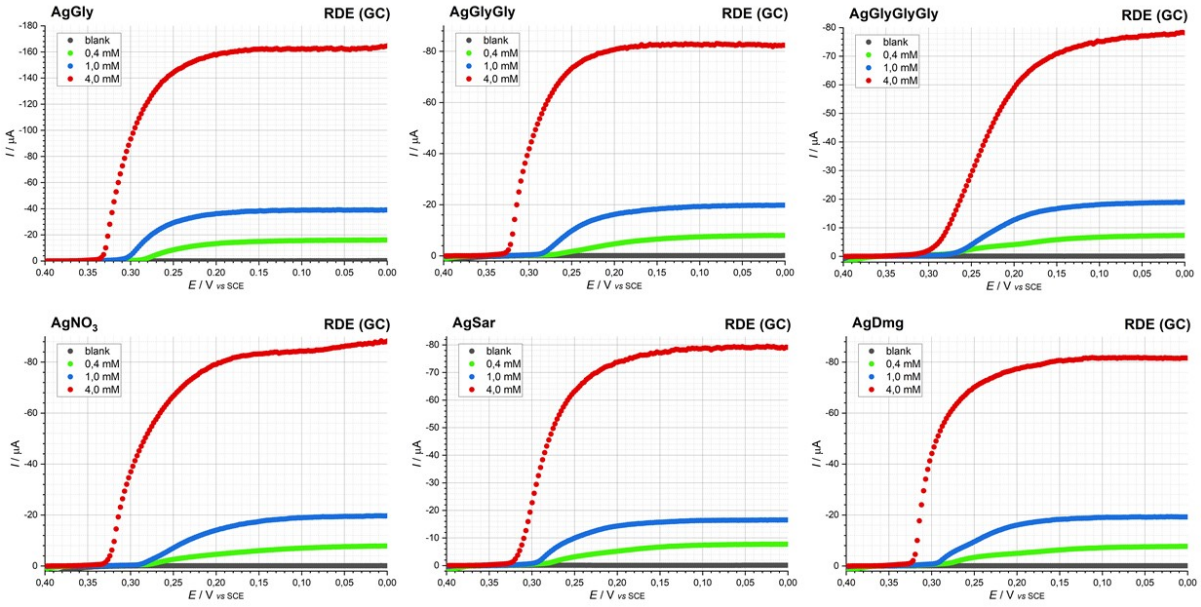

Figure S22 RDE voltammetry (GC electrode) of the studied Ag(I) compounds measured in the defined concentration values of the solutions 0.4, 1.0 and 4.0 mM

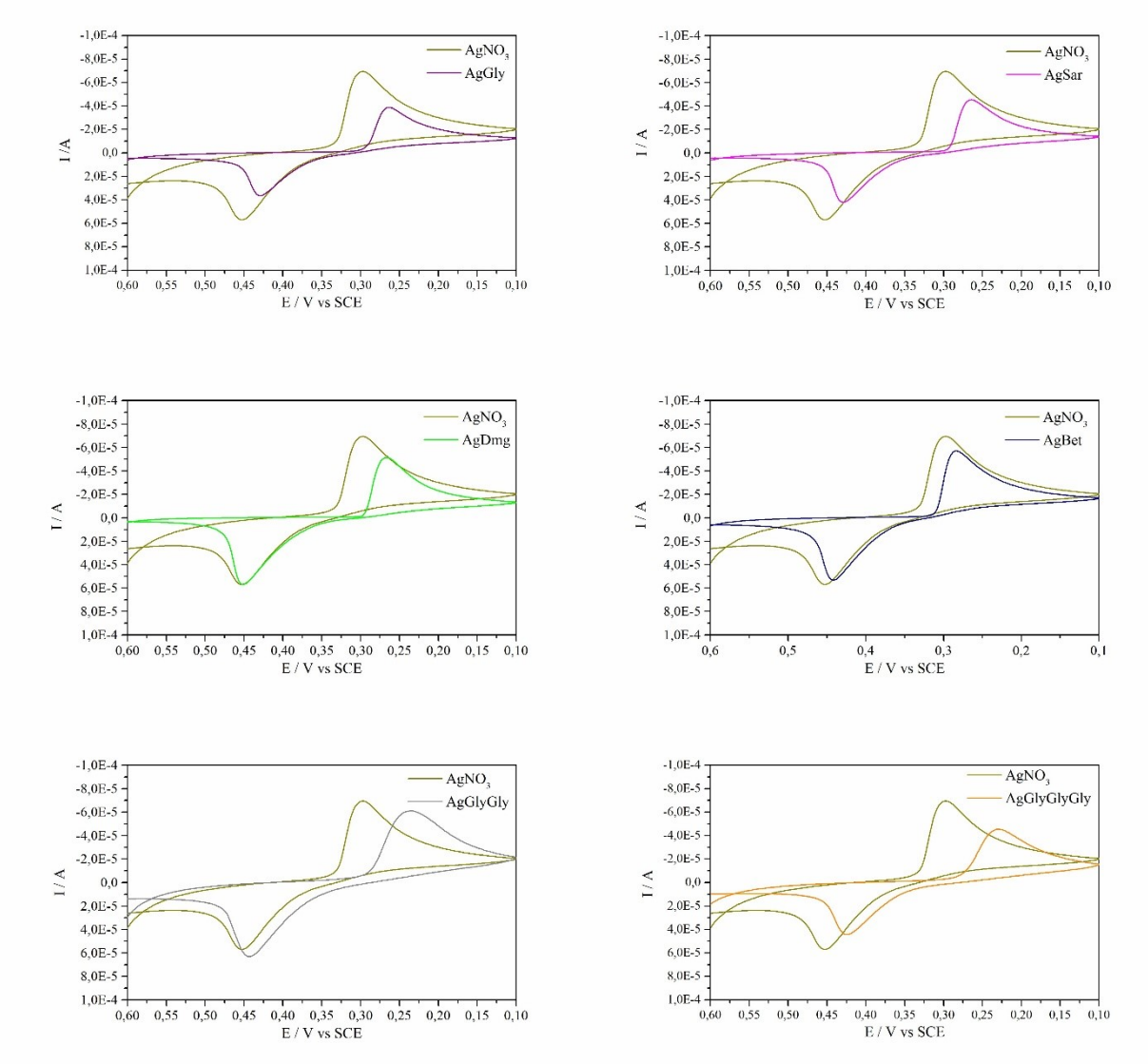

Figure S23 CV voltammetry (GC electrode) of the studied Ag(I) compounds measured in the concentration range of the solutions 0.75–2.89 mM

RPMI + complex/ligand

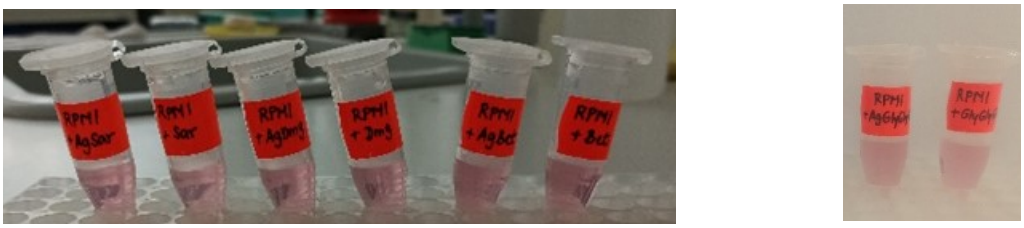

RPMI (SA) + complex/ligand

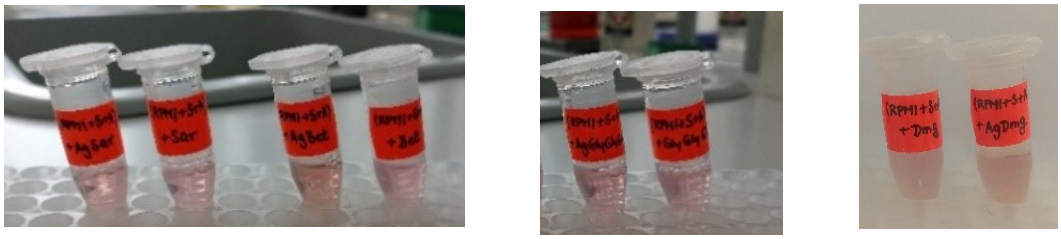

SB + complex/ligand

MHB + complex/ligand

Figure S24 Samples after incubation

RPMI + complex/ligand/$AgNO_3$/DMSO

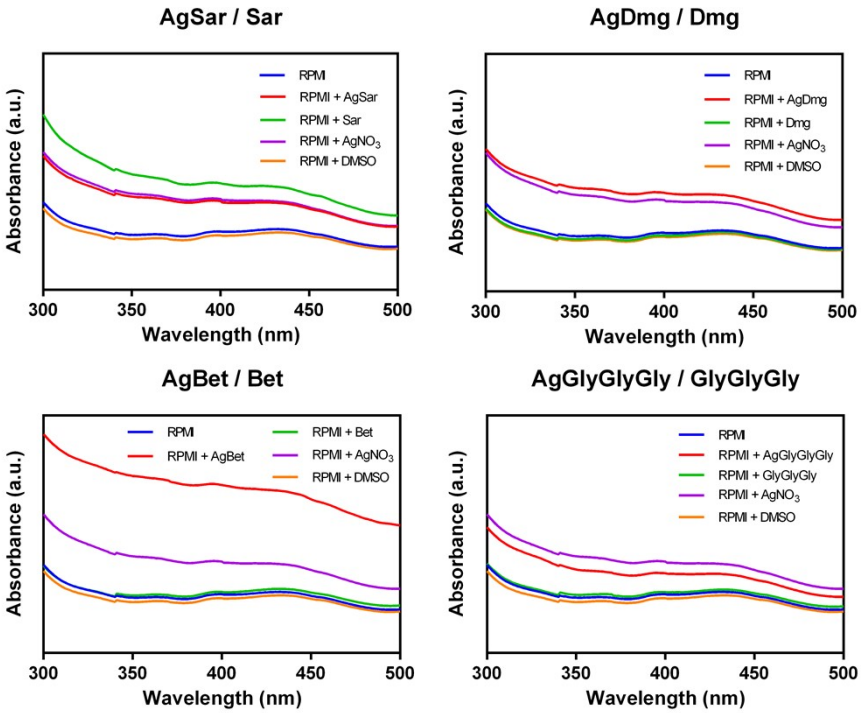

RPMI(SA) + complex/ligand/$AgNO_3$/DMSO

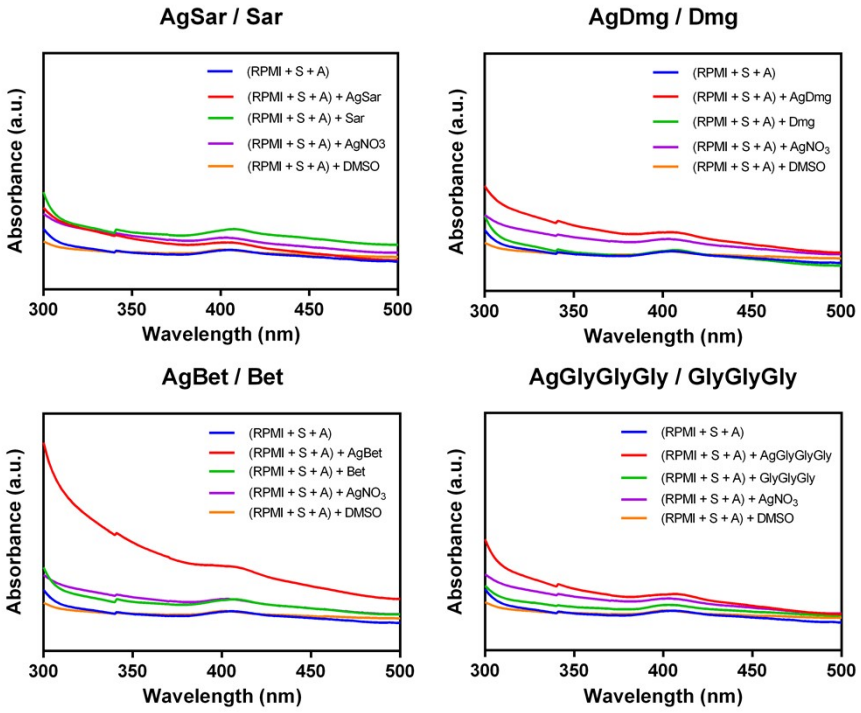

SB + complex/ligand/$AgNO_3$

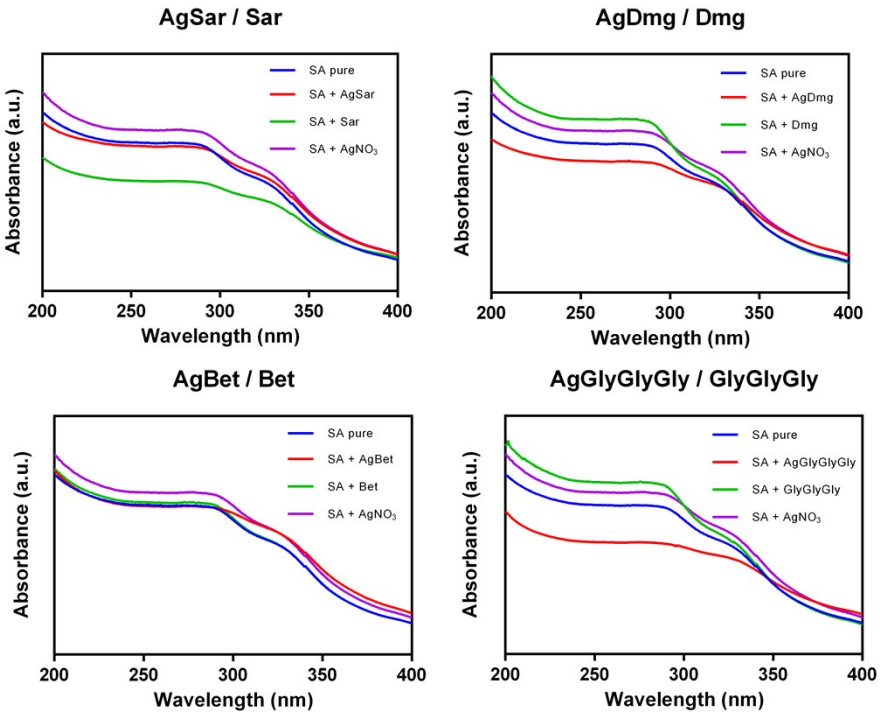

MHB + complex/ligand/$AgNO_3$

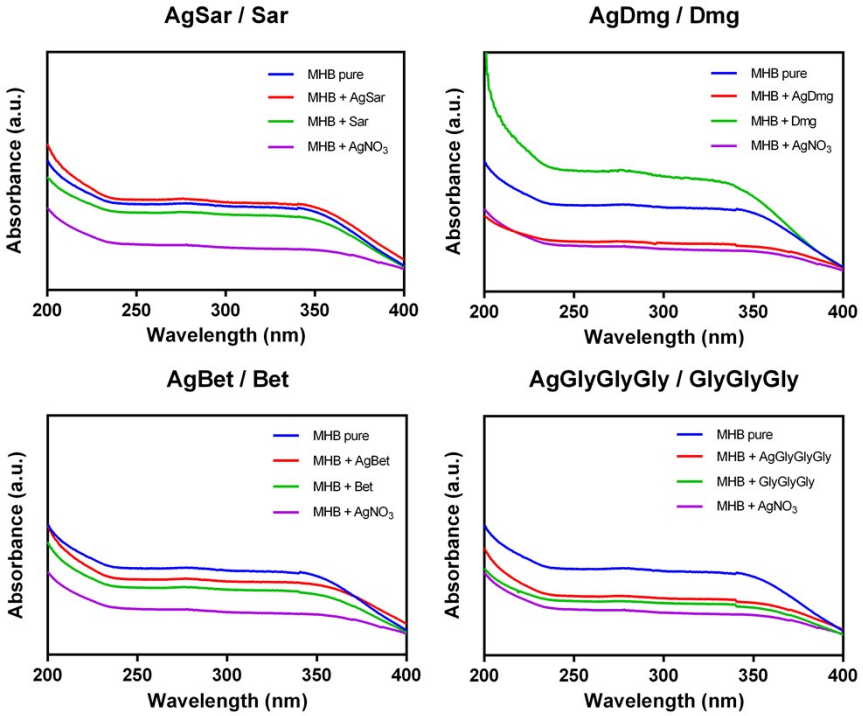

Figure S25 UV-Vis spectra of **RPMI** + complex/ligand/$AgNO_3$/DMSO; (**RPMI(SA)**) + complex/ligand/$AgNO_3$/DMSO; **SB** + complex/ligand/$AgNO_3$; **MHB** + complex/ligand/$AgNO_3$; (*c*(complex/ligand/$AgNO_3$ = 100 μM)

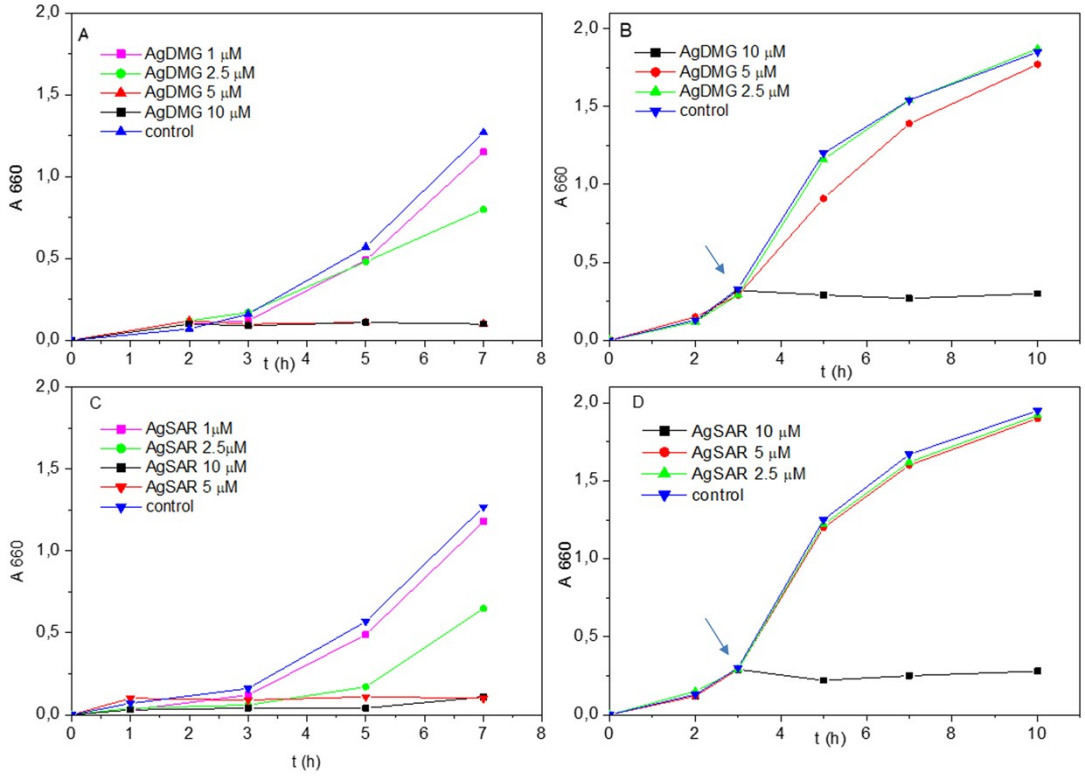

Figure S26 The growth of *S. aureus* in the presence of AgDmg (A, B) AgSar (C, D) after addition to lag phase (A, C) or to the exponential growth phase (B, D), The arrow indicates the addition of the silver complex

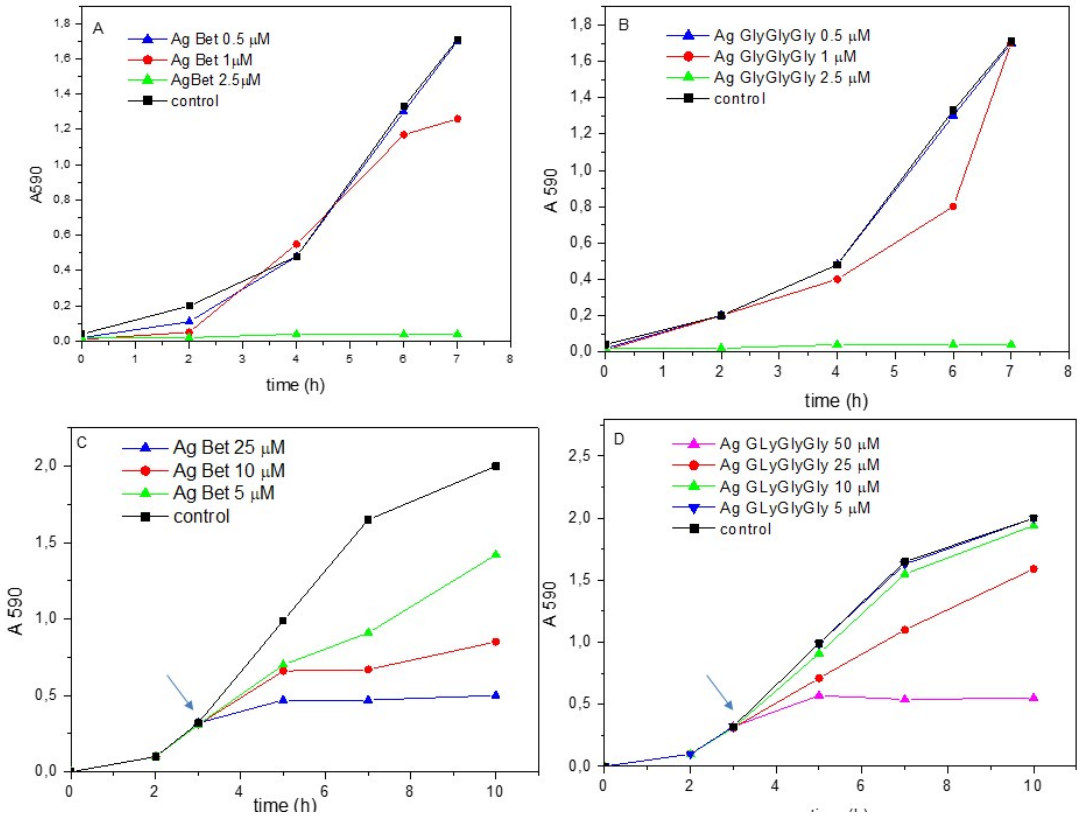

Figure S27 The growth of *S. aureus* in the presence of AgBet (A, C) AgGlyGlyGly (B, D) after addition to lag phase (A, B) or to the exponential growth phase (C, D), The arrow indicates the addition of the silver complex

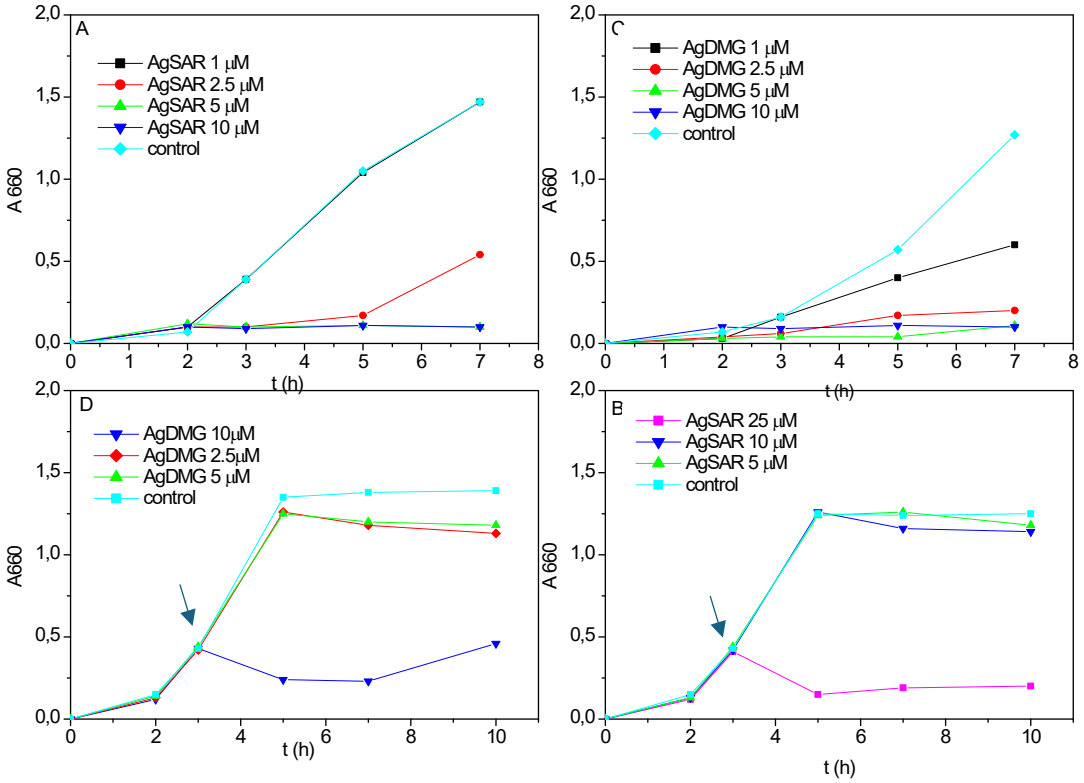

Figure S28 The growth of *E. coli* in the presence of AgDmg (C, D) Ag Sar (A, B) after addition to lag phase (A, B) or to the exponential growth phase (C, D), The arrow indicates the addition of the silver complex

Figure S29 The growth of *E. coli* in the presence of AgBet (A, C) AgGlyGlyGly (B, D) after addition to lag phase (A, B) or to the exponential growth phase (C, D), The arrow indicates the addition of the silver complex

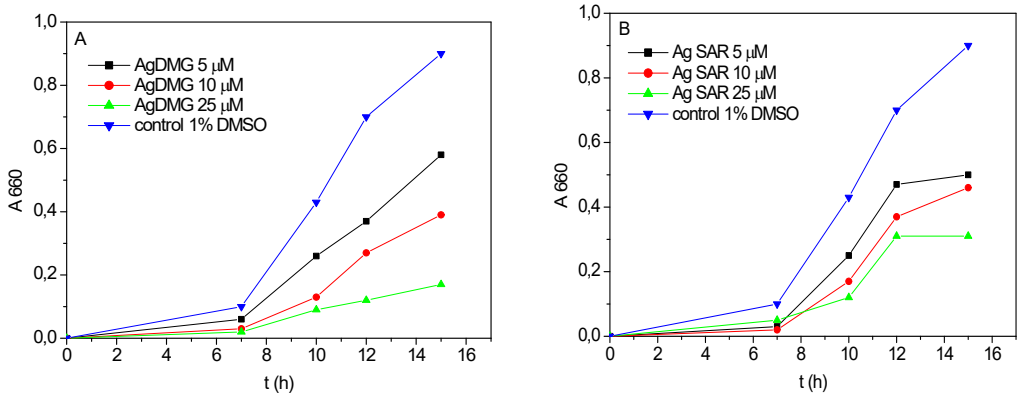

Figure S30 The growth of *C. parapsilosis* in the presence of AgDmg (A) AgSar (B) after addition to lag phase

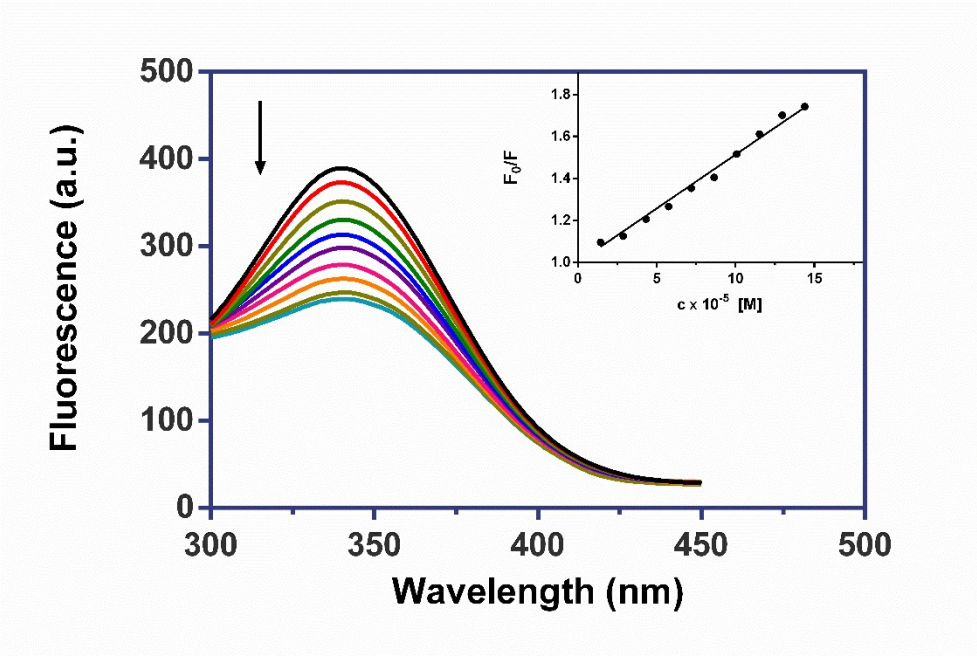

Figure S31 Fluorescence spectra of HSA upon the addition of complex AgGlyGlyGly in 10 mM Phosphate-buffered saline (pH = 7.4). Inset: Stern-Volmer plot

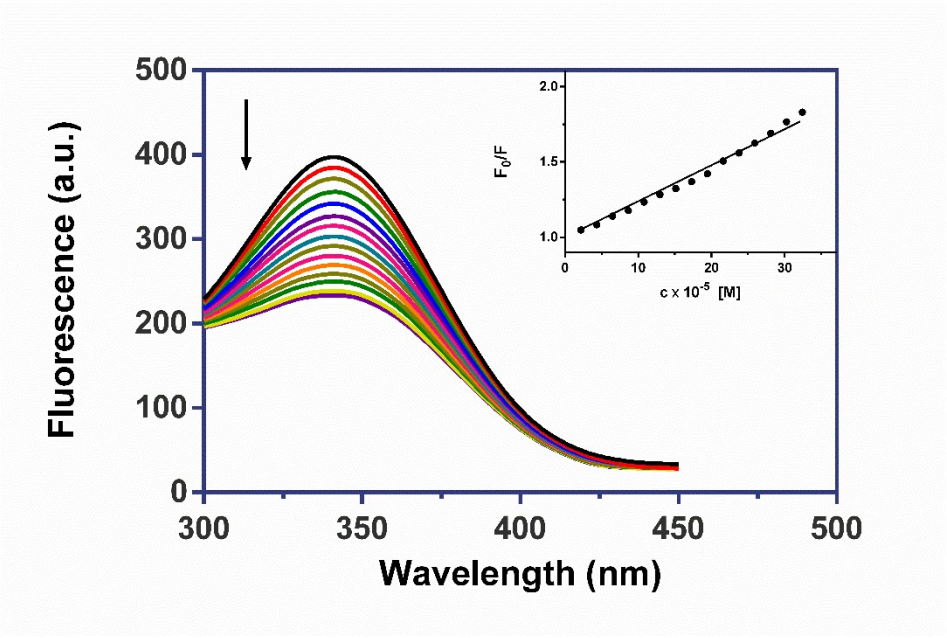

Figure S32 Fluorescence spectra of HSA upon the addition of complex AgDmg in 10 mM Phosphate-buffered saline (pH = 7.4). Inset: Stern-Volmer plot

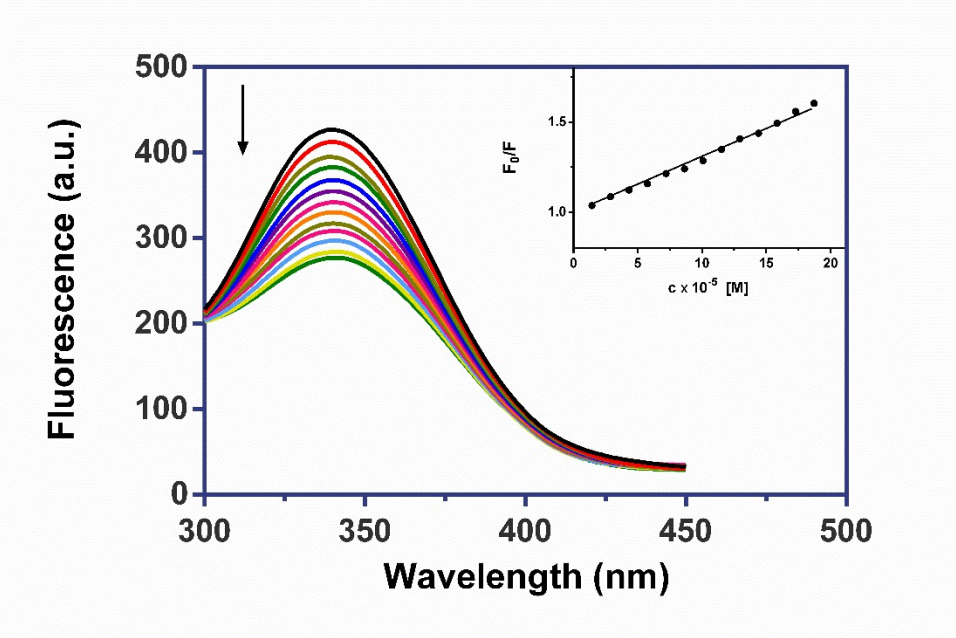

Figure S33 Fluorescence spectra of HSA upon the addition of complex AgSar in 10 mM Phosphate-buffered saline (pH = 7.4). Inset: Stern-Volmer plot

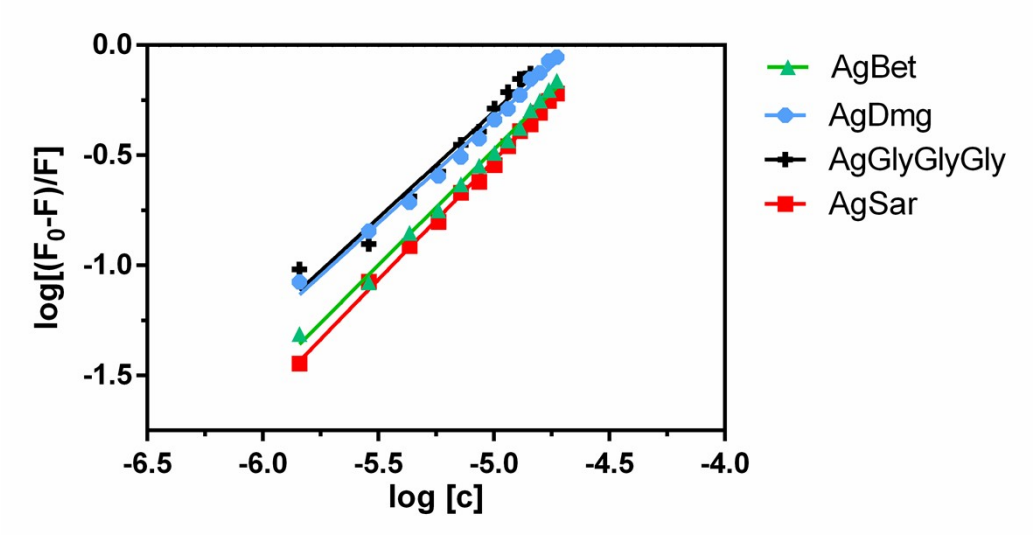

Figure S34 Modified Stern-Volmer plots related to binding of the complexes AgBet, AgDmg, AgGlyGlyGly and AgSar to HSA

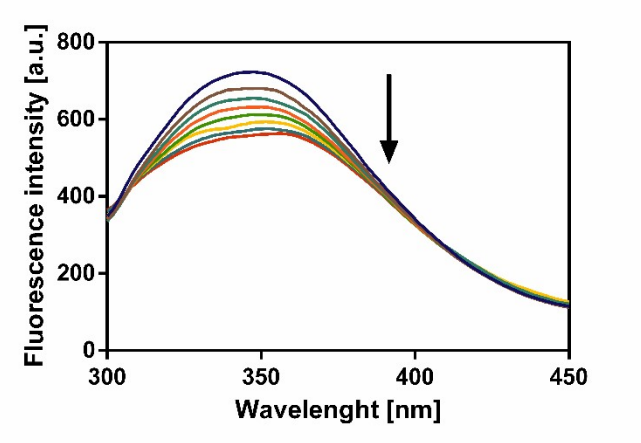

Figure S35A Fluorescence spectra of HSA-WAR system upon the addition of complex AgSar

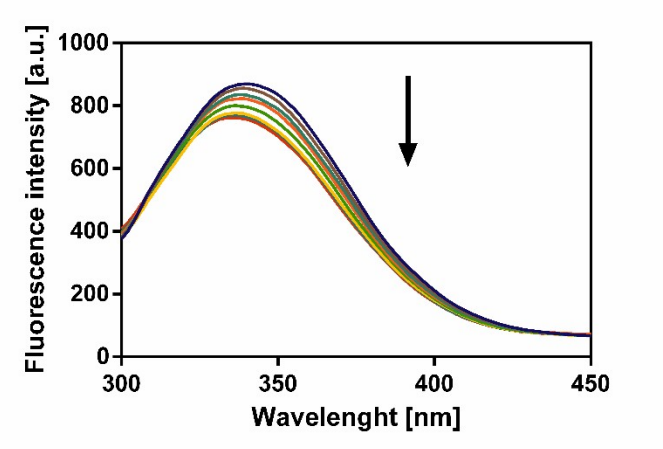

Figure S35B Fluorescence spectra of HSA-IBU system upon the addition of complex AgSar

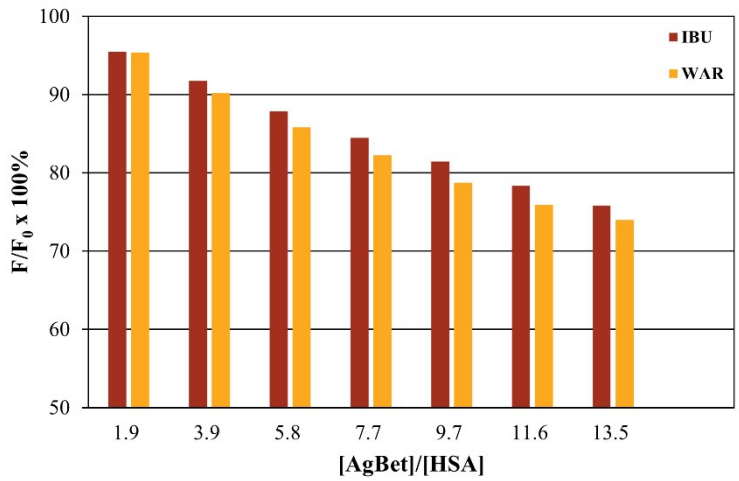

Figure S36 Bar graph for complex AgBet presenting site markers displacement assay by ibuprofen (IBU) and warfarin (WAR).

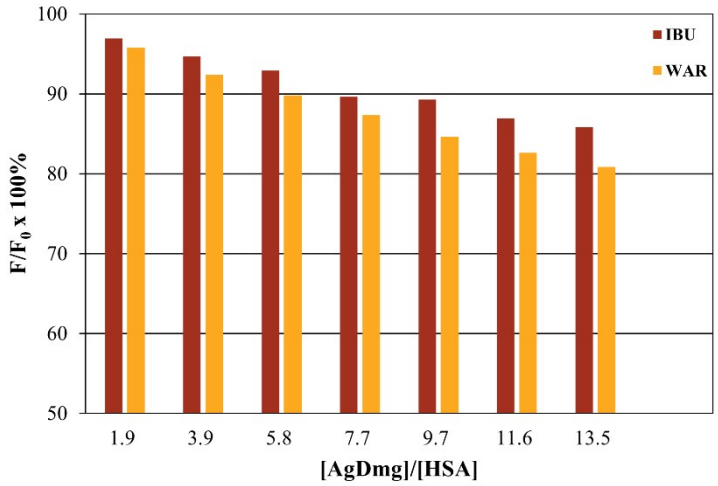

Figure S37 Bar graph for complex AgDmg presenting site markers displacement assay by ibuprofen (IBU) and warfarin (WAR).

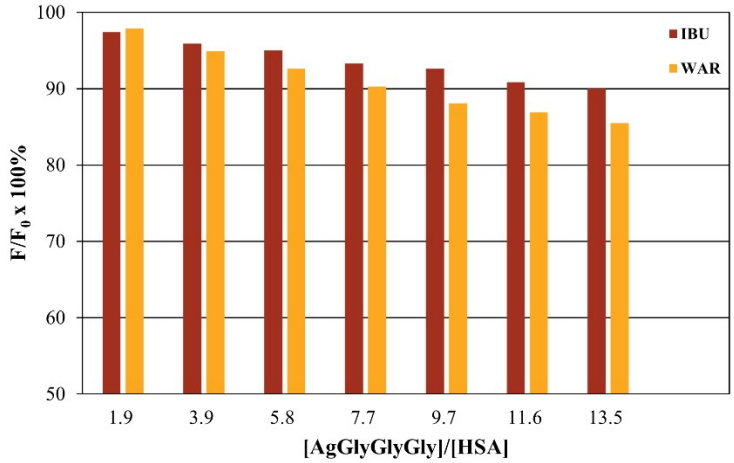

Figure S38 Bar graph for complex AgGlyGlyGly presenting site markers displacement assay by ibuprofen (IBU) and warfarin (WAR).

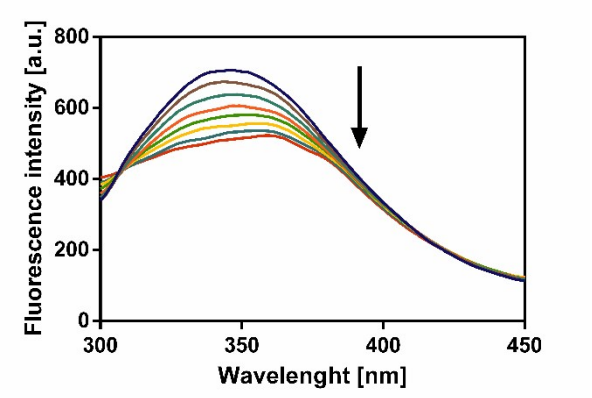

Figure S39A Fluorescence spectra of HSA-WAR system upon the addition of complex AgBet

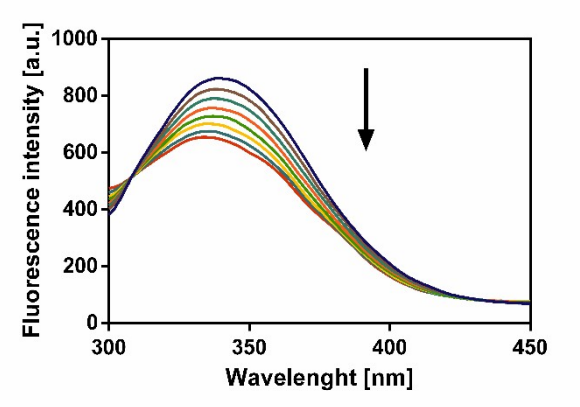

Figure S39B Fluorescence spectra of HSA-IBU system upon the addition of complex AgBet

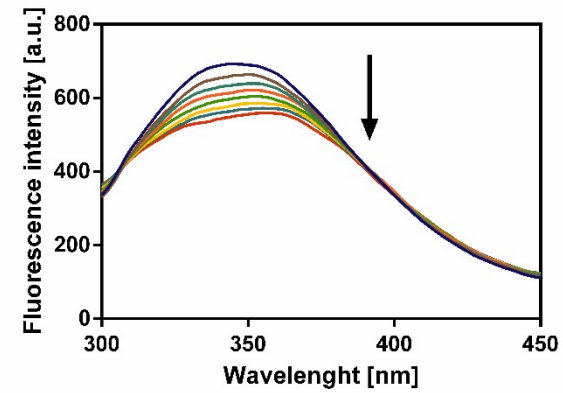

Figure S40A Fluorescence spectra of HSA-WAR system upon the addition of complex AgDmg

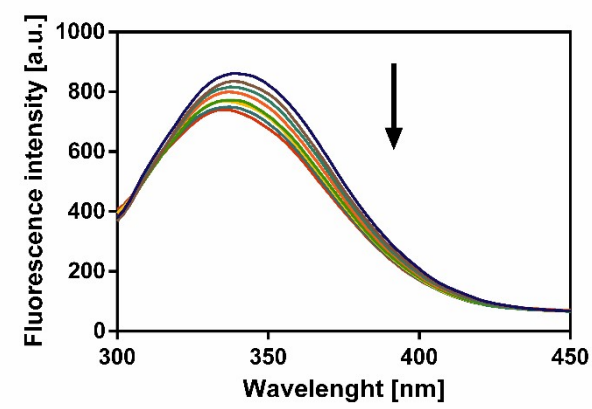

Figure S40B Fluorescence spectra of HSA-IBU system upon the addition of complex AgDmg

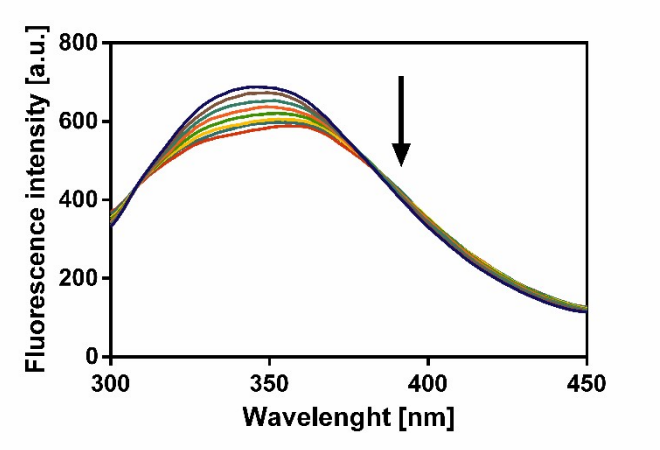

Figure S41A Fluorescence spectra of HSA-WAR system upon the addition of complex AgGlyGlyGly

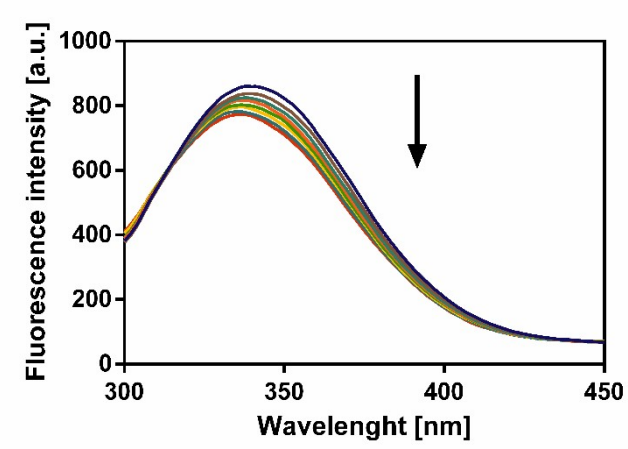

Figure S41B Fluorescence spectra of HSA-IBU system upon the addition of complex AgGlyGlyGly

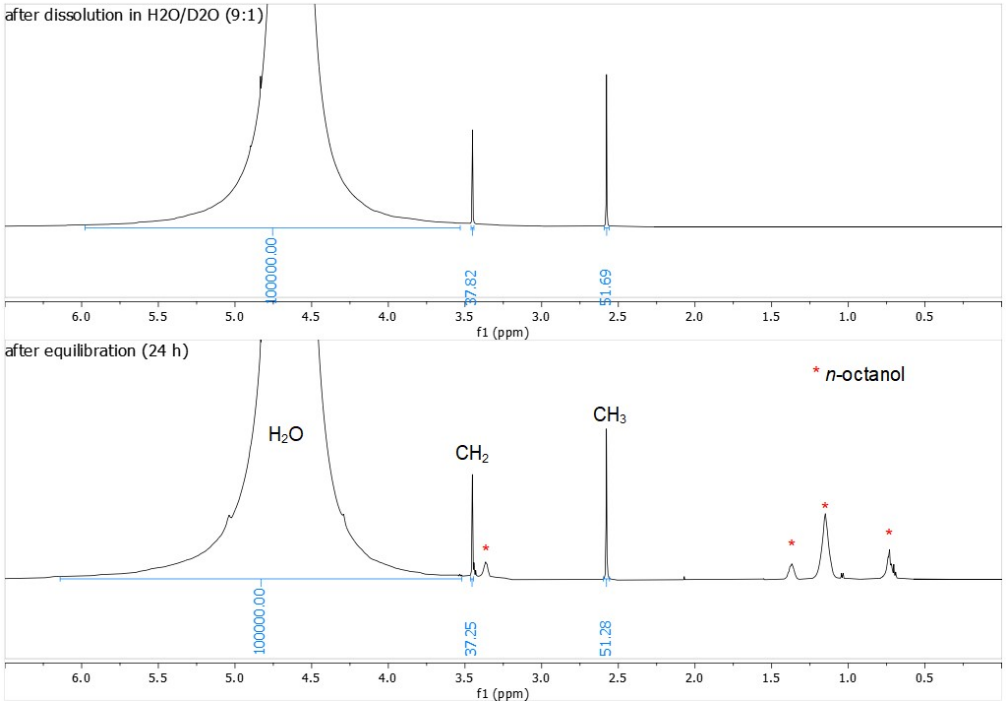

Figure S42 ^{1}H NMR (600 MHz) spectra of complex AgSar before and after equilibration

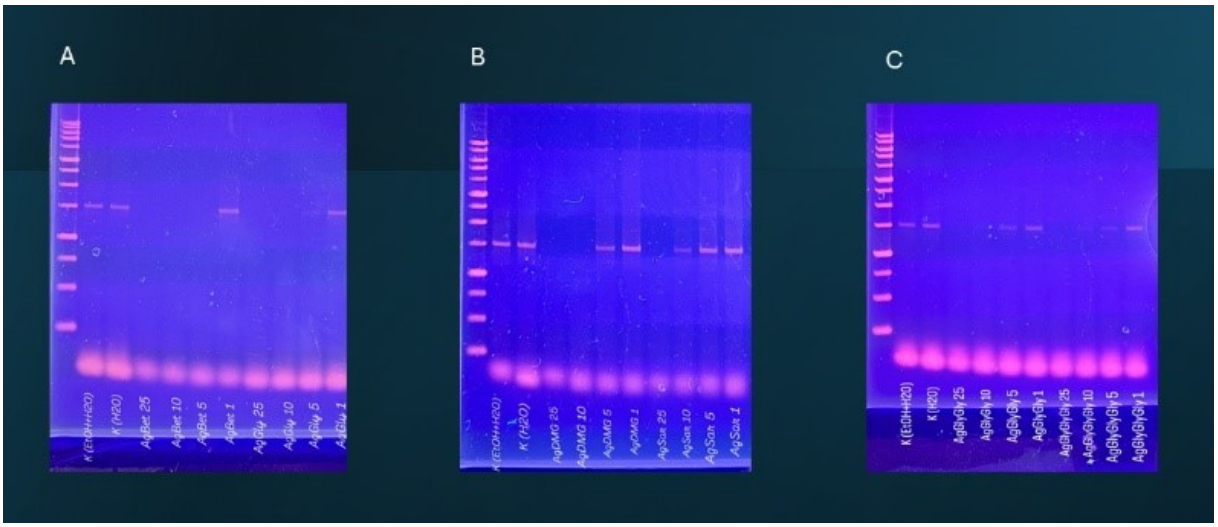

Figure S43 Inhibition of PCR amplification by silver(I) complexes.

A–C. Agarose gel electrophoresis showing the effect of increasing concentrations of silver complexes on the amplification of the ~1400 bp 16S rDNA fragment using Taq DNA polymerase. Control reactions (K; EtOH/H_2O and H_2O) produced a strong and distinct PCR product. In contrast, all silver complexes caused a concentration-dependent suppression of amplification.

A. Complexes AgBet and AgGly (25 -1 μM)

B. Complexes AgDmg and AgSar (25 -1 μM)

C. Complexes AgGlyGlyGly and AgGlyGly (25 -1 μM)

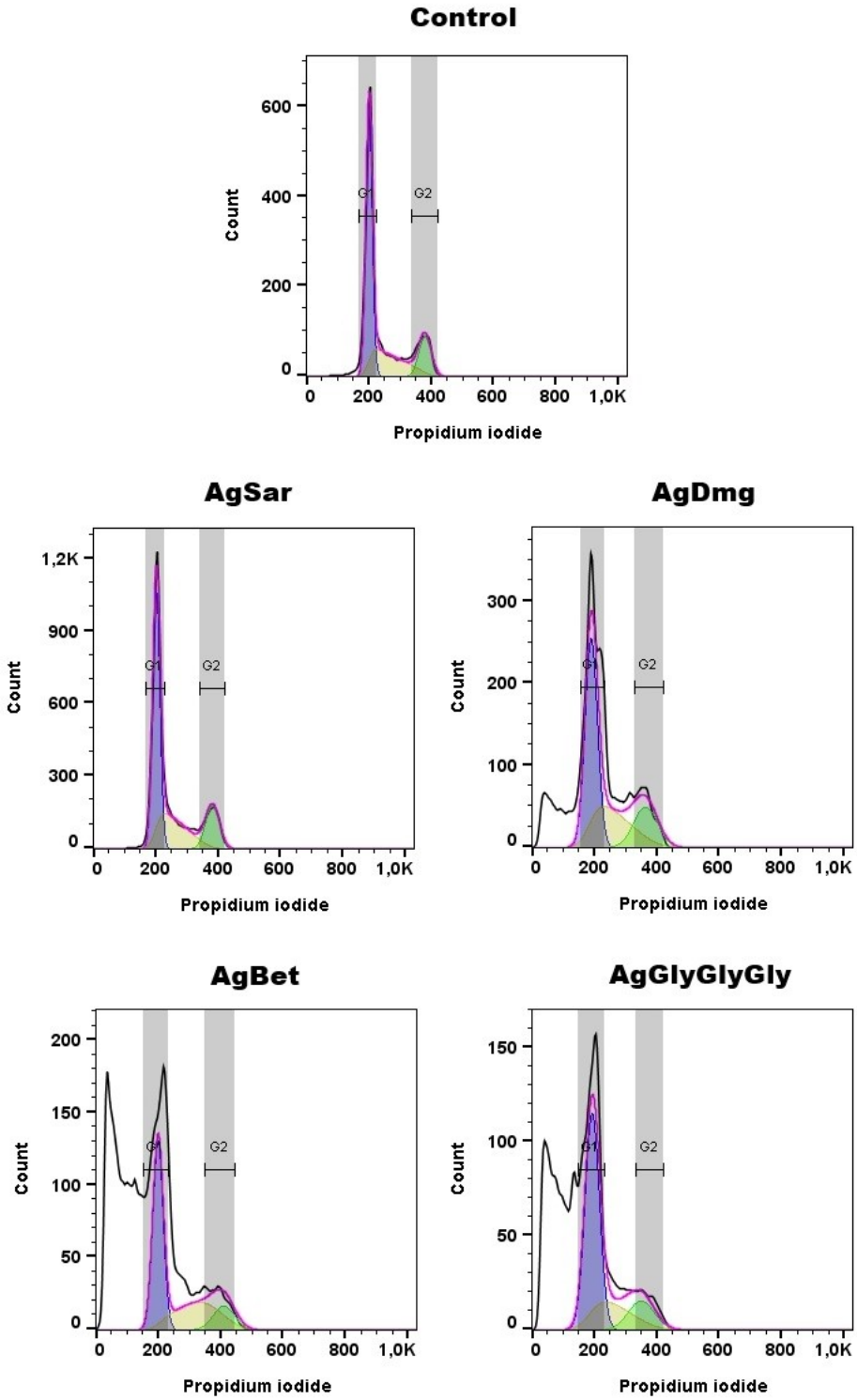

Figure S44 Representative histograms of cell cycle distribution of MDA-MB-231 cells after 24 h treatment with Ag(I) complexes.

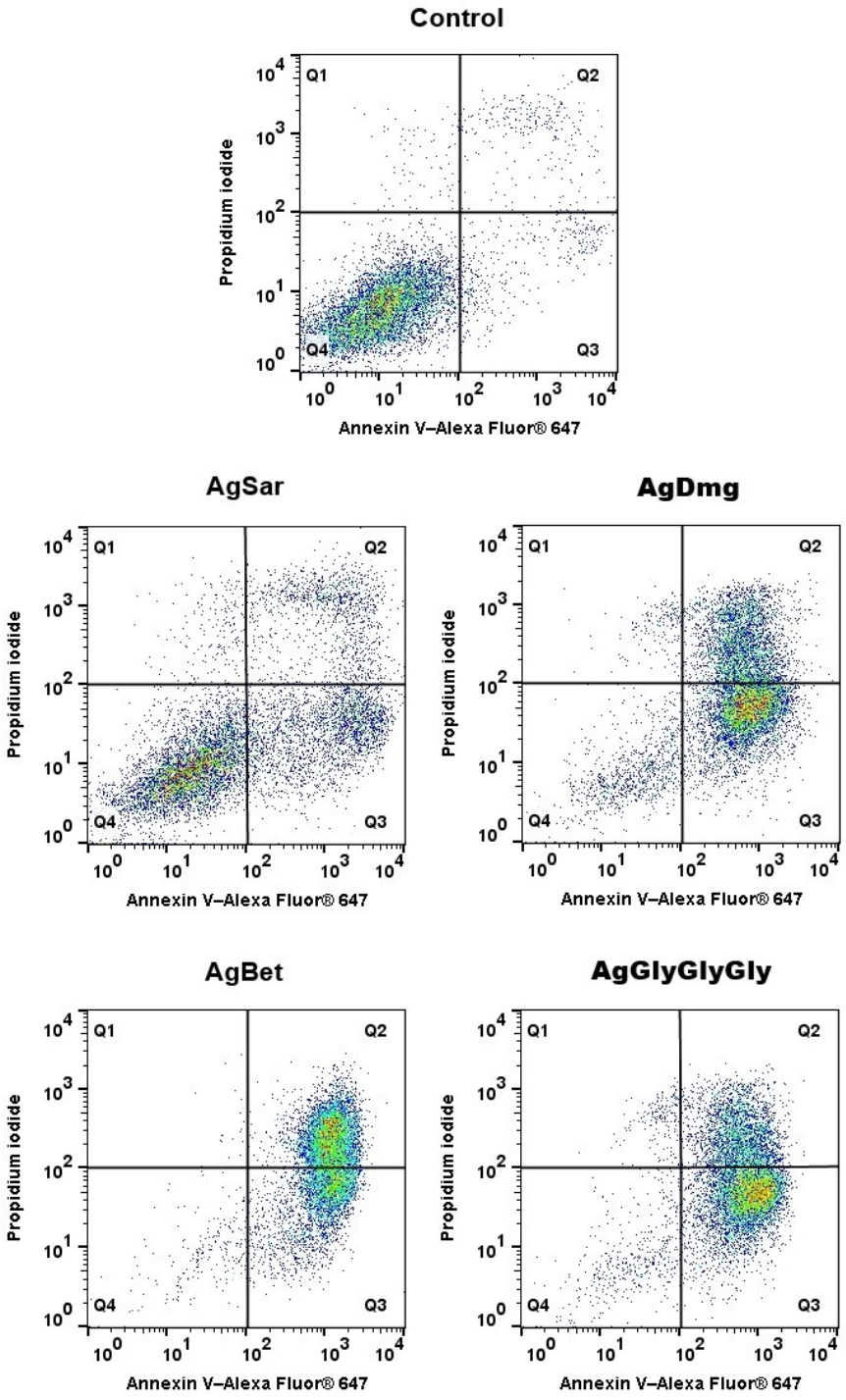

Figure S45 representative dot plots of Annexin V/Pi staining of MDA-MB-231 cells after 24 h treatment with Ag(I) complexes

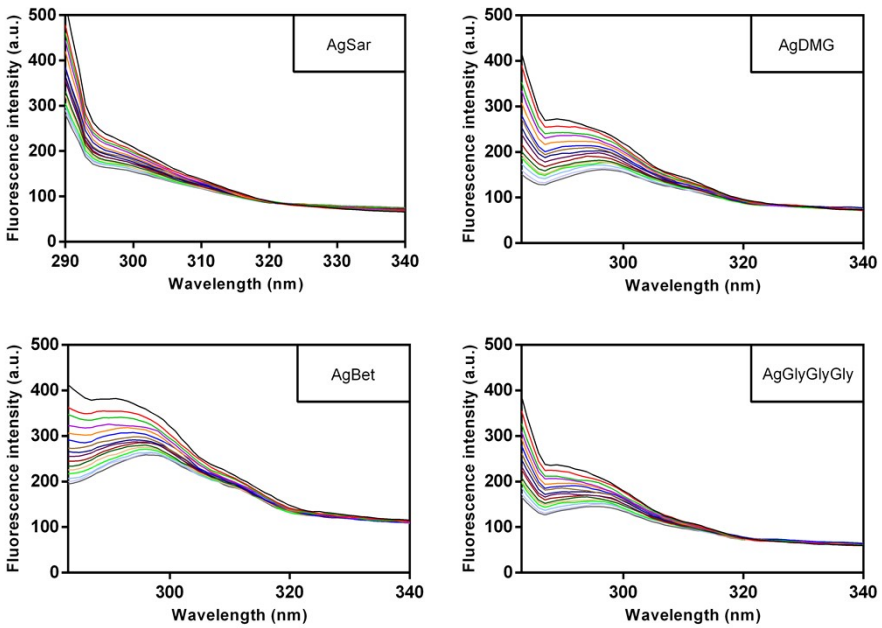

Figure S46 Spectrofluorimetric titration of silver(I) complexes (AgSar, AgDmg, AgBet, AgGlyGlyGly) with ctDNA (0–21.41 μM) in Tris-HCl buffer (pH 7.4) at 21 ± 1 °C. Initial silver(I) complex concentration: 49.75 μM (black line).

Table S1 Crystal data and structure refinement for silver(I) complexes.

	AgSar	**AgDmg**	**AgBet**
Empirical formula	$C_3H_7AgN_2O_5$	$C_4H_9AgN_2O_5$	$C_{10}H_{22}Ag_3N_5O_{13}$
Formula weight	258.98	273.00	743.93
Temperature [K]	120(2)	120(2)	120(2)
Wavelength [Å]	0.71073	0.71073	0.71073
Crystal system	Monoclinic	Monoclinic	Orthorhombic
Space group	$P2_1/n$	$P2_1/c$	$P2_12_12$
Unit cell dimensions	a = 5.9666(3)	a = 5.5261(4)	a = 15.7832(8)
[Å, °]	b = 8.4114(4)	b = 11.2082(8)	b = 23.2072(12)
	c = 13.8333(6)	c = 14.0565(12)	c = 5.6320(2)
	α = 90	α = 90	α = 90
	β = 101.712(2)	β = 97.992(3)	β = 90
	γ = 90	γ = 90	γ = 90
Volume [Å^3]	679.80(6)	862.17(11)	2062.91(17)
Z	4	2	4
Calculated density [g.cm^{-3}]	2.530	2.319	2.395
Absorption coefficient [mm^{-1}]	2.942	2.346	2.895
F (000)	504	592	1448
Crystal size [mm^3]	0.530 x 0.213 x 0.084	0.171 x 0.162 x 0.058	0.270 x 0.178 x 0.116
θ range for data collection [°]	3.506 – 28.302	2.333 – 26.489	2.581 – 28.297
Index ranges	$-7 \le h \le 7$, $-11 \le k \le 11$, $-18 \le l \le 18$	$-6 \le h \le 6$, $-14 \le k \le 14$, $-17 \le l \le 17$	$-21 \le h \le 21$, $-30 \le k \le 30$, $-7 \le l \le 7$
Reflections collected/unique	12879 / 1685	31594 / 3526	47613 / 5135
Data / restraints / parameters	1685 / 12 / 108	3526 / 17 / 267	5135 / 0 / 286
Completeness to theta = 25.242° [%]	99.8	99.7	99.9
Max. and min. transmission	0.79 and 0.20	0.73 and 0.54	0.73 and 0.57

Goodness-of-fit on F^2	1.115	1.108	1.068
Final R indices [$I > 2\sigma(I)$]	$R1$ = 0.0150; $wR2$ = 0.0348	$R1$ = 0.0351; $wR2$ = 0.1062	$R1$ = 0.0154; $wR2$ = 0.0374
R indices (all data)	$R1$ = 0.0164; $wR2$ = 0.0353	$R1$ = 0.0358; $wR2$ = 0.1071	$R1$ = 0.0157; $wR2$ = 0.0375
Largest diff. peak and hole [e.Å^{-3}]	0.473, -0.492	2.396, -1.008	0.638 , -0.513

Table S2 Bond distances (Å) and angles (°) for **AgSar**

Bond distances		**Bond angles**	
Ag(1)-O(2)	2.2221(10)	O(2)-Ag(1)-O(1)^{i}	148.66(4)
Ag(1)-O(1)^{i}	2.2770(10)	O(2)-Ag(1)-O(3)	114.95(4)
Ag(1)-O(3)	2.4094(11)	O(1)^{i} -Ag(1)-O(3)	86.40(4)
Ag(1)-Ag(1)^{i}	2.8462(2)	O(2)-Ag(1)-Ag(1)^{i}	77.76(3)
O(1)-C(1)	1.2631(19)	O(1)^{i} -Ag(1)-Ag(1)^{i}	81.77(3)
C(1)-O(2)	1.2485(18)	O(3)-Ag(1)-Ag(1)^{i}	167.29(3)
C(1)-C(2)	1.518(2)	C(1)-O(1)-Ag(1)^{i}	116.67(9)
C(2)-N(1)	1.484(2)	O(2)-C(1)-O(1)	126.79(14)
C(2)-H(2A)	0.9900	O(2)-C(1)-C(2)	117.64(13)
C(2)-H(2B)	0.9900	O(1)-C(1)-C(2)	115.53(13)
N(1)-C(3)	1.4938(19)	C(1)-O(2)-Ag(1)	123.36(10)
N(1)-H(1N1)	0.88(2)	N(1)-C(2)-C(1)	112.67(12)
N(1)-H(2N1)	0.89(2)	N(1)-C(2)-H(2A)	109.1
C(3)-H(3A)	0.9800	C(1)-C(2)-H(2A)	109.1
C(3)-H(3B)	0.9800	N(1)-C(2)-H(2B)	109.1
C(3)-H(3C)	0.9800	C(1)-C(2)-H(2B)	109.1
N(2)-O(4)	1.2533(17)	H(2A)-C(2)-H(2B)	107.8
N(2)-O(3)	1.2542(17)	C(2)-N(1)-C(3)	113.15(12)
N(2)-O(5)	1.2554(17)	C(2)-N(1)-H(1N1)	113.1(14)
		C(3)-N(1)-H(1N1)	108.4(14)
		C(2)-N(1)-H(2N1)	107.8(13)
		C(3)-N(1)-H(2N1)	108.8(13)
		H(1N1)-N(1)-H(2N1)	105.3(18)
		N(1)-C(3)-H(3A)	109.5
		N(1)-C(3)-H(3B)	109.5
		H(3A)-C(3)-H(3B)	109.5
		N(1)-C(3)-H(3C)	109.5
		H(3A)-C(3)-H(3C)	109.5
		H(3B)-C(3)-H(3C)	109.5
		O(4)-N(2)-O(3)	120.42(13)
		O(4)-N(2)-O(5)	119.93(13)
		O(3)-N(2)-O(5)	119.65(13)
		N(2)-O(3)-Ag(1)	116.13(9)

Symmetry codes: (i) -x, -y+1, -z+1

Table S3 Possible hydrogen bonds (Å, °) for **AgSar**

D-H...A	d(D-H)	d(H...A)	d(D...A)	<(DHA)
C(2)-H(2A)...O(2)^{ii}	0.99	2.40	3.0786(18)	125
C(2)-H(2B)...O(5)^{iii}	0.99	2.46	3.1951(19)	130
N(1)-H(1N1)...O(1)^{iv}	0.88(2)	1.99(2)	2.8474(17)	166(2)
N(1)-H(2N1)...O(5)^{v}	0.89(2)	1.98(2)	2.8556(17)	168.6(18)
C(3)-H(3A)...O(2)	0.98	2.44	3.001(2)	116
C(3)-H(3A)...O(4)	0.98	2.60	3.4657(19)	148
C(3)-H(3B)...O(3)^{vi}	0.98	2.37	3.203(2)	142

Symmetry codes: (ii) -x+1/2,y+1/2,-z+3/2; (iii) x-1/2,-y+1/2,z+1/2; (iv) -x+1/2,y-1/2,-z+3/2;

(v) -x+3/2, y+1/2, -z+3/2; (vi) x+1/2, -y+1/2, z+1/2

Table S4 Bond distances (Å) and angles (°) for **AgDmg**

Bond distances		Bond angles	
Ag(1)-O(2)	2.2628(10)	O(2)-Ag(1)-O(1)^{i}	152.06(4)
Ag(1)-O(1)^{i}	2.3000(10)	O(2)-Ag(1)-O(2)^{ii}	78.84(4)
Ag(1)-O(2)^{ii}	2.4293(11)	O(1)^{i}-Ag(1)-O(2)^{ii}	104.81(4)
Ag(1)-O(3)	2.4388(11)	O(2)-Ag(1)-O(3)	116.86(4)
Ag(1)-Ag(1)^{i}	2.9057(2)	O(1)^{i}-Ag(1)-O(3)	81.90(4)
O(1)-C(1)	1.2443(18)	O(2)^{ii}-Ag(1)-O(3)	131.63(4)
C(1)-O(2)	1.2622(17)	O(2)-Ag(1)-Ag(1)^{i}	79.20(3)
C(1)-C(2)	1.5301(18)	O(1)^{i}-Ag(1)-Ag(1)^{i}	80.71(3)
C(2)-N(1)	1.4931(17)	O(2)^{ii}-Ag(1)-Ag(1)^{i}	139.12(3)
C(2)-H(2A)	0.9900	O(3)-Ag(1)-Ag(1)^{i}	89.13(3)
C(2)-H(2B)	0.9900	C(1)-O(1)-Ag(1)^{i}	117.58(9)
N(1)-C(3)	1.4914(18)	O(1)-C(1)-O(2)	127.05(13)
N(1)-C(4)	1.4952(17)	O(1)-C(1)-C(2)	118.66(12)
N(1)-H(1)	0.87(2)	O(2)-C(1)-C(2)	114.28(12)
C(3)-H(3A)	0.9800	C(1)-O(2)-Ag(1)	124.28(9)
C(3)-H(3B)	0.9800	C(1)-O(2)-Ag(1)^{ii}	132.03(9)
C(3)-H(3C)	0.9800	Ag(1)-O(2)-Ag(1)^{ii}	101.16(4)
C(4)-H(4A)	0.9800	N(1)-C(2)-C(1)	112.63(11)
C(4)-H(4B)	0.9800	N(1)-C(2)-H(2A)	109.1
C(4)-H(4C)	0.9800	C(1)-C(2)-H(2A)	109.1
N(2)-O(4)	1.2495(16)	N(1)-C(2)-H(2B)	109.1
N(2)-O(3)	1.2540(16)	C(1)-C(2)-H(2B)	109.1
N(2)-O(5)	1.2564(16)	H(2A)-C(2)-H(2B)	107.8
		C(3)-N(1)-C(2)	112.93(11)
		C(3)-N(1)-C(4)	110.17(11)
		C(2)-N(1)-C(4)	110.42(11)
		C(3)-N(1)-H(1)	108.0(13)
		C(2)-N(1)-H(1)	109.1(13)
		C(4)-N(1)-H(1)	105.9(13)
		N(1)-C(3)-H(3A)	109.5

N(1)-C(3)-H(3B)	109.5
H(3A)-C(3)-H(3B)	109.5
N(1)-C(3)-H(3C)	109.5
H(3A)-C(3)-H(3C)	109.5
H(3B)-C(3)-H(3C)	109.5
N(1)-C(4)-H(4A)	109.5
N(1)-C(4)-H(4B)	109.5
H(4A)-C(4)-H(4B)	109.5
N(1)-C(4)-H(4C)	109.5
H(4A)-C(4)-H(4C)	109.5
H(4B)-C(4)-H(4C)	109.5
O(4)-N(2)-O(3)	120.35(12)
O(4)-N(2)-O(5)	120.13(12)
O(3)-N(2)-O(5)	119.53(12)
N(2)-O(3)-Ag(1)	111.07(9)

Symmetry codes: (i) -x+1, -y+1, -z+1; (ii) -x+2, -y+1, -z+1

Table S5 Possible hydrogen bonds (Å, °) for **AgDmg**

D-H...A	**d(D-H)**	**d(H...A)**	**d(D...A)**	**<(DHA)**
C(2)-H(2B)...O(4)^{ii}	0.99	2.46	3.4179(19)	162
N(1)-H(1)...N(2)^{iii}	0.87(2)	2.566(19)	3.3755(17)	155.7(17)
N(1)-H(1)...O(4)^{iii}	0.87(2)	2.517(18)	3.1545(17)	131.0(16)
N(1)-H(1)...O(5)^{iii}	0.87(2)	1.96(2)	2.8093(16)	166.8(18)
C(3)-H(3B)...O(3)^{iv}	0.98	2.53	3.4035(19)	148
C(3)-H(3C)...O(1)	0.98	2.45	3.0311(18)	117
C(4)-H(4B)...O(5)^{v}	0.98	2.45	3.2776(19)	142
C(4)-H(4C)...O(3)^{iv}	0.98	2.42	3.3144(19)	152

Symmetry codes: (ii) -x+2, -y+1, -z+1; (iii) x, -y+1/2, z+1/2; (iv) -x+1, y+1/2, -z+3/2;

(v) x+1, -y+1/2, z+1/2

Table S6 Bond distances (Å) and angles (°) for **AgBet**

Bond distances		**Bond angles**	
Ag(1)-O(3)	2.195(2)	O(3)-Ag(1)-O(2)	157.76(8)
Ag(1)-O(2)	2.283(2)	O(3)-Ag(1)-O(4)^{i}	112.32(7)
Ag(1)-O(4)^{i}	2.450(2)	O(2)-Ag(1)-O(4)^{i}	83.96(7)
Ag(1)-Ag(2)	2.8678(3)	O(3)-Ag(1)-Ag(2)	82.68(6)
Ag(1)-Ag(1)^{ii}	2.9917(5)	O(2)-Ag(1)-Ag(2)	80.43(5)
Ag(2)-O(1)	2.207(2)	O(4)^{i}-Ag(1)-Ag(2)	164.39(5)
Ag(2)-O(4)	2.329(2)	O(3)-Ag(1)-Ag(1)^{ii}	127.88(6)
Ag(2)-O(2)^{iii}	2.413(2)	O(2)-Ag(1)-Ag(1)^{ii}	60.19(5)
Ag(2)-O(5)	2.588(2)	O(4)^{i}-Ag(1)-Ag(1)^{ii}	98.54(5)
Ag(2)-Ag(2)^{ii}	2.9074(5)	Ag(2)-Ag(1)-Ag(1)^{ii}	73.904(7)
Ag(3)-O(9)	2.451(2)	O(1)-Ag(2)-O(4)	159.68(8)
Ag(3)-O(6)	2.452(3)	O(1)-Ag(2)-O(2)^{iii}	113.94(7)

Ag(3)-O(5)^{i}	2.472(2)	O(4)-Ag(2)-O(2)^{iii}	83.81(7)
Ag(3)-O(11)	2.559(3)	O(1)-Ag(2)-O(5)	92.56(8)
O(1)-C(1)	1.245(3)	O(4)-Ag(2)-O(5)	75.45(8)
O(2)-C(1)	1.266(3)	O(2)^{iii}-Ag(2)-O(5)	94.73(7)
C(1)-C(2)	1.515(4)	O(1)-Ag(2)-Ag(1)	82.70(6)
C(2)-N(1)	1.505(3)	O(4)-Ag(2)-Ag(1)	79.38(5)
C(2)-H(2A)	0.9900	O(2)^{iii}-Ag(2)-Ag(1)	163.18(5)
C(2)-H(2B)	0.9900	O(5)-Ag(2)-Ag(1)	81.54(6)
N(1)-C(3)	1.500(4)	O(1)-Ag(2)-Ag(2)^{ii}	121.07(6)
N(1)-C(4)	1.503(4)	O(4)-Ag(2)-Ag(2)^{ii}	63.09(5)
N(1)-C(5)	1.509(3)	O(2)^{iii}-Ag(2)-Ag(2)^{ii}	96.80(5)
C(3)-H(3A)	0.9800	O(5)-Ag(2)-Ag(2)^{ii}	135.23(6)
C(3)-H(3B)	0.9800	Ag(1)-Ag(2)-Ag(2)^{ii}	75.198(7)
C(3)-H(3C)	0.9800	O(9)-Ag(3)-O(6)	108.87(8)
C(4)-H(4A)	0.9800	O(9)-Ag(3)-O(5)^{i}	128.49(8)
C(4)-H(4B)	0.9800	O(6)-Ag(3)-O(5)^{i}	89.87(7)
C(4)-H(4C)	0.9800	O(9)-Ag(3)-O(11)	138.12(8)
C(5)-H(5A)	0.9800	O(6)-Ag(3)-O(11)	101.20(9)
C(5)-H(5B)	0.9800	O(5)^{i}-Ag(3)-O(11)	78.75(9)
C(5)-H(5C)	0.9800	C(1)-O(1)-Ag(2)	123.93(19)
O(3)-C(6)	1.238(4)	C(1)-O(2)-Ag(1)	120.25(17)
O(4)-C(6)	1.258(3)	C(1)-O(2)-Ag(2)^{i}	135.97(18)
C(6)-C(7)	1.535(4)	Ag(1)-O(2)-Ag(2)^{i}	97.24(7)
C(7)-N(2)	1.503(3)	O(1)-C(1)-O(2)	126.3(3)
C(7)-H(7A)	0.9900	O(1)-C(1)-C(2)	120.1(2)
C(7)-H(7B)	0.9900	O(2)-C(1)-C(2)	113.6(2)
N(2)-C(8)	1.500(4)	N(1)-C(2)-C(1)	116.6(2)
N(2)-C(10)	1.502(4)	N(1)-C(2)-H(2A)	108.1
N(2)-C(9)	1.507(4)	C(1)-C(2)-H(2A)	108.1
C(8)-H(8A)	0.9800	N(1)-C(2)-H(2B)	108.1
C(8)-H(8B)	0.9800	C(1)-C(2)-H(2B)	108.1
C(8)-H(8C)	0.9800	H(2A)-C(2)-H(2B)	107.3
C(9)-H(9A)	0.9800	C(3)-N(1)-C(4)	110.4(2)
C(9)-H(9B)	0.9800	C(3)-N(1)-C(2)	111.3(2)
C(9)-H(9C)	0.9800	C(4)-N(1)-C(2)	111.1(2)
C(10)-H(10A)	0.9800	C(3)-N(1)-C(5)	108.3(2)
C(10)-H(10B)	0.9800	C(4)-N(1)-C(5)	108.1(2)
C(10)-H(10C)	0.9800	C(2)-N(1)-C(5)	107.5(2)
N(3)-O(7)	1.241(3)	N(1)-C(3)-H(3A)	109.5
N(3)-O(6)	1.254(4)	N(1)-C(3)-H(3B)	109.5
N(3)-O(5)	1.263(4)	H(3A)-C(3)-H(3B)	109.5
N(4)-O(10)	1.236(3)	N(1)-C(3)-H(3C)	109.5
N(4)-O(8)	1.245(3)	H(3A)-C(3)-H(3C)	109.5
N(4)-O(9)	1.263(3)	H(3B)-C(3)-H(3C)	109.5
N(5)-O(12)	1.241(3)	N(1)-C(4)-H(4A)	109.5
N(5)-O(13)	1.246(4)	N(1)-C(4)-H(4B)	109.5
N(5)-O(11)	1.247(4)	H(4A)-C(4)-H(4B)	109.5
		N(1)-C(4)-H(4C)	109.5
		H(4A)-C(4)-H(4C)	109.5

H(4B)-C(4)-H(4C)	109.5
N(1)-C(5)-H(5A)	109.5
N(1)-C(5)-H(5B)	109.5
H(5A)-C(5)-H(5B)	109.5
N(1)-C(5)-H(5C)	109.5
H(5A)-C(5)-H(5C)	109.5
H(5B)-C(5)-H(5C)	109.5
C(6)-O(3)-Ag(1)	123.95(19)
C(6)-O(4)-Ag(2)	117.62(18)
C(6)-O(4)-Ag(1)^{iii}	137.03(18)
Ag(2)-O(4)-Ag(1)^{iii}	94.99(7)
O(3)-C(6)-O(4)	127.2(3)
O(3)-C(6)-C(7)	119.1(3)
O(4)-C(6)-C(7)	113.7(2)
N(2)-C(7)-C(6)	116.3(2)
N(2)-C(7)-H(7A)	108.2
C(6)-C(7)-H(7A)	108.2
N(2)-C(7)-H(7B)	108.2
C(6)-C(7)-H(7B)	108.2
H(7A)-C(7)-H(7B)	107.4
C(8)-N(2)-C(10)	108.8(2)
C(8)-N(2)-C(7)	112.1(2)
C(10)-N(2)-C(7)	107.3(2)
C(8)-N(2)-C(9)	110.0(2)
C(10)-N(2)-C(9)	107.7(2)
C(7)-N(2)-C(9)	110.8(2)
N(2)-C(8)-H(8A)	109.5
N(2)-C(8)-H(8B)	109.5
H(8A)-C(8)-H(8B)	109.5
N(2)-C(8)-H(8C)	109.5
H(8A)-C(8)-H(8C)	109.5
H(8B)-C(8)-H(8C)	109.5
N(2)-C(9)-H(9A)	109.5
N(2)-C(9)-H(9B)	109.5
H(9A)-C(9)-H(9B)	109.5
N(2)-C(9)-H(9C)	109.5
H(9A)-C(9)-H(9C)	109.5
H(9B)-C(9)-H(9C)	109.5
N(2)-C(10)-H(10A)	109.5
N(2)-C(10)-H(10B)	109.5
H(10A)-C(10)-H(10B)	109.5
N(2)-C(10)-H(10C)	109.5
H(10A)-C(10)-H(10C)	109.5
H(10B)-C(10)-H(10C)	109.5
O(7)-N(3)-O(6)	120.7(3)
O(7)-N(3)-O(5)	119.8(3)
O(6)-N(3)-O(5)	119.5(2)
N(3)-O(5)-Ag(3)^{iii}	102.41(18)
N(3)-O(5)-Ag(2)	118.50(19)

Ag(3)^{iii}-O(5)-Ag(2)	130.52(10)
N(3)-O(6)-Ag(3)	106.06(18)
O(10)-N(4)-O(8)	121.3(3)
O(10)-N(4)-O(9)	119.8(3)
O(8)-N(4)-O(9)	118.9(3)
N(4)-O(9)-Ag(3)	101.41(18)
O(12)-N(5)-O(13)	121.0(3)
O(12)-N(5)-O(11)	118.7(3)
O(13)-N(5)-O(11)	120.3(3)
N(5)-O(11)-Ag(3)	98.25(19)

Symmetry codes: (i) x, y, z+1; (ii) -x+1, -y+1, z ; (iii) x, y, z-1

Table S7 Possible hydrogen bonds (Å, °) for **AgBet**

D-H...A	**d(D-H)**	**d(H...A)**	**d(D...A)**	**<(DHA)**
C(2)-H(2B)...O(11)	0.99	2.42	3.343(4)	155
C(3)-H(3B)...O(1)	0.98	2.34	2.973(4)	121
C(4)-H(4A)...O(9)^{iv}	0.98	2.36	3.259(4)	153
C(4)-H(4C)...O(1)	0.98	2.32	2.931(4)	120
C(5)-H(5B)...O(12)^{v}	0.98	2.35	3.268(4)	155
C(7)-H(7B)...O(8)^{iii}	0.99	2.58	3.453(4)	147
C(8)-H(8A)...O(10)^{vi}	0.98	2.43	3.327(4)	152
C(8)-H(8B)...N(5)^{vii}	0.98	2.59	3.556(4)	170
C(8)-H(8C)...O(3)	0.98	2.28	2.920(4)	122
C(9)-H(9A)...O(3)	0.98	2.35	2.977(4)	121
C(9)-H(9A)...O(8)	0.98	2.49	3.089(4)	119
C(9)-H(9B)...O(8)^{iii}	0.98	2.50	3.386(4)	150
C(9)-H(9C)...O(10)^{vi}	0.98	2.54	3.402(4)	147
C(10)-H(10B)...O(8)^{iii}	0.98	2.60	3.461(4)	147
C(10)-H(10C)...O(13)^{vii}	0.98	2.38	3.279(4)	153

Symmetry codes: (iii) x, y, z-1; (iv) x-1/2, -y+3/2, -z+1; (v) x-1/2, -y+3/2, -z+2; (vi) -x+2, -y+1, z; (vii) -x+3/2, y-1/2, -z+1

Table S8 IR spectral data assignments [cm^{-1}] for free ligands and their appropriate silver(I) complexes [*21 **17 +38].

	Sar	**AgSar**	**Dmg**	**AgDmg**	**Bet**	**AgBet**	**GlyGlyGly**	**AgGlyGlyGly**	**Gly*+**	**AgGly*+**	**GlyGly****	**AgGlyGly**+**
ν(NH) + ν(CH)	3247	–	3400–2400	3100–2400	3400–2800	3400–2800	3400–2400	3300–2500	3300-2400	3400-2400	3350–2500	3350–2500
ν(CH)	3031	3029										
ν (C=O)	–	–	–	–	–	–	1678	1668				
δ $(NH_2)_{scissor.}$	1642	–	–	–	–	–	1639	1634	–	–	1653	1645
ν_{as} (COO^-)	1603	1568	1595	1585	1613	1581	1514	1538	1525	1593	1572	1522
ν_s (COO^-)	1436	1414	1423	1417	1409	1446	1392	1416	1413	1488	1478	1446
Δ (ν_{as}– ν_s)	–	154	–	168	–	135	–	122	–	105	–	76
δ $(CH_3)_{as}$	1471	1472	1478	1479	1486	1485	–	–	–	–	–	–
δ (CH_2)	–	1456	1454	–	1457	–	1434	1456	–	–		
δ $(CH_3)_s$	1401	1392	1375	1398	1384	1381	–	–	–	–		
ν (NO_3^-)	–	1315	–	1317	–	1310	–	1293	–	1320	–	1316
tw (CH_2)	1281	–	1278	–	1236	–	1290	1272	–	–	–	–
ν (CN)/ ν $C(H_3)N$	1147	1151	1135	1174	1143,1130	1135	1159, 1122	1121	–	–	–	–
ν $(CCN)_{alif.}$ + γ (CH_3)	1062	1063	1061	1022	1011	1035	1078	1040	1032	1034	1096	1077
	993	944	991	993	984	980	989	979	–	–	–	–
ν (CC)	973, 892	865,817	986, 866	960, 861	935, 890	921, 823	907, 884	906, 814	891	892	964,916	907,824
δ $(COO^-)_{scissor.}$	697	680	696	–	707	598	688, 645	675	–	–	588,528	598,548
δ $(COO^-)_{rocking}$	482	452	508	460	442	452	464	467	–	–	–	–

Abbreviation: ν – stretching, δ – bending, tw – twisting, γ – out-of-plane bending

Table S9 The binding constants K_b of fluorescence quenching of HSA- IBU/WAR system by silver(I) complexes

complex	**AgSar**	**AgBet**	**AgDmg**	**AgGlyGlyGly**
$K_b \times 10^3 [M^{-1}]$ **IBU**	14.23	6.65	10.21	4.71
$K_b \times 10^3 [M^{-1}]$ **WAR**	0.76	9.53	8.45	7.04